1-1-2018

Improving the Detection Limit of Tau Aggregates for Use with Biological Samples

Emily Rickman Hager
University of Denver

IMPROVING THE DETECTION LIMIT OF TAU AGGREGATES FOR USE WITH BIOLOGICAL SAMPLES

_____

A Thesis

Presented to

the Faculty of Natural Sciences and Mathematics

University of Denver

_____

In Partial Fulfillment

of the Requirements for the Degree

Master of Science

_____

by

Emily Rickman Hager

March 2018

Advisor: Martin Margittai

Author: Emily Rickman Hager
Title: IMPROVING THE DETECTION LIMIT OF TAU AGGREGATES FOR USE WITH BIOLOGICAL SAMPLES
Advisor: Martin Margittai
Degree Date: March 2018

Abstract

The protein Tau is found in neurofibrillary tangles in Alzheimer's disease and over 20 other neurodegenerative diseases. An assay has been developed to detect minute amounts of fibrils from human brain tissue. This assay subjects brain tissue extract and recombinant Tau to several rounds of sonication and incubation. Incubation allows recombinant Tau to add itself to the ends of the existing fibrils in brain tissue extract. Sonication breaks the existing fibrils in the brain tissue extract offering more ends for Tau to add onto. Cycles of sonication and incubation have been shown to allow for amplification of Tau fibrils from Alzheimer's disease tissue. This assay can be used not only for detection, but also to note differences between tauopathies and to look at various agents that have been shown to block fibril growth.

Acknowledgements

First, I would like to thank Dr. Martin Margittai for your constant guidance and direction. I would also like to thank Dr. David Patterson, Dr. Michelle Knowles, and Dr. Mark Siemans for your encouragement and participation on my committee since year one. To the entire Molecular and Cellular Biophysics program, thank you for accepting me into the program in its infancy and offering the opportunity for collaboration and friendship among different disciplines.

Thanks to my lab gang, Michael Holden, Hilary Weismiller, and Justin Shady. You've been my collaborators, comedians, and sushi consumers. Things didn't always go exactly as planned, but having you around improved my graduate school experience

Thank you to my family for working together through the long hours, inconvenient scheduling, and stress that a graduate program introduced into our lives. I love you all. Mom and Dad, thank you for teaching me that I could grow up to be anything I wanted. Janet, thank you for demonstrating to me that it isn't necessary to be a traditional student to find success. To Ro, I know that you believed in me from the beginning, and that has helped me through. Brian, thank you most of all. You are the one who wouldn't let me quit. You stuck with me through all of the tears, stress, and anxiety and never doubted me. I am grateful to each and every one of you.

Table of Contents

List of Figures

List of Abbreviations

3R	three-repeat
4R	four-repeat
AA	amino acid
AD	Alzheimer's Disease
APP	Amyloid Precursor Protein
Aβ	Amyloid-β
BCA	bicinchoninic acid
BSE	Bovine spongiform encephalopathy
CJD	Creutzfeldt-Jakob Disease
cl	cystiene-less
CR	Congo Red
CTE	Chronic Traumatic Encephalopathy
DS	Down Syndrome
DTT	dithiothreitol
E. coli	*Escherichia coli*
EDTA	Ethylenediaminetetraacetic acid
EM	Electron Microscopy
FFI	Fatal Familial Insomnia
FTDP17	Frontotemporal Dementia with Parkinsonism linked to Chromosome 17
HEPES	4-(2-Hydrosyethyl)piperazine-1-ethanesulfonic acid
IPTG	isopropyl β-D-1-thiogalactopyranoside

LB	Luria Bertani Broth
MAP	microtubule associated protein
ME	monomer equivalent
NaCl	Sodium chloride
NaN_3	Sodium azide
NFT	Neurofibrillary Tangle
OD600	Optical Density at 600nm
PAGE	Polyacrylamide Gel Electrophoresis
PiD	Pick's Disease
PIPES	piperazine-N,N'-bis(2-ethanesulfonic acid)
PK	Proteinase K
PMSF	phenylmethane sulfonyl fluoride
PrP	Prion Protein
PrP^{SC}	Misfolded Prion Protein
PSP	Progressive Supranuclear Palsey
RTQuIC	Real-Time Quaking Induced Conversion
SDS	Sodium dodecyl sulfate
TCEP	Tris(2-Carboxyethyl)phosphine Hydrochloride
ThT	Thioflavin T
TrMAP2	Truncated MAP2
vCJD	Variant Creutzfeldt-Jakob disease

Chapter One: Introduction

1.1 Protein Aggregation Diseases

1.1.1 Discovery of Diseases of Protein Aggregation

Protein aggregates in the form of amyloid plaques and neurofibrillary tangles (NFTs) have been observed in Alzheimer's Disease (AD) since 1906 when Alois Alzheimer first described the disease, which was later named for him[1]. The identified amyloid plaques were eventually discovered to be composed of the peptide Amyloid-β (Aβ)[2] and the tangles consist of the protein Tau[3]. The cause of these plaques and tangles was unknown, but they were seen repeatedly in the brain tissue of AD patients, along with significant neurodegeneration and loss of grey matter and white matter[4].

The discovery of Prion protein (PrP) aggregates in scrapie sheep introduced the idea that protein aggregates could be the infectious agent in disease[5]. Prion diseases occur in a variety of mammals including chronic wasting disease in cervid populations[6], bovine spongiform encephalopathy (BSE) in cows[7], and scrapie in sheep. Creutzfeldt-Jakob disease (CJD), fatal familial insomnia (FFI), kuru and other prion diseases are known to occur in humans[8]. For many years, prion diseases were thought to be caused by a "slow virus" [9]. First scrapie and then Kuru were identified as infectious diseases with long incubation times and similar pathologies[9]. The evidence provided was that an injection of scrapie infected material into the brain of a healthy sheep caused infection, but only over

time. The rationale was that this is caused by a virus with an incubation time of months to years. In 1986[10], Ashley T. Haase suggested that AD was similar in progress and lengthy incubation time to these other slow viruses, but was unable to identify a specific infectious agent, thus suggesting the term "unconventional agent" be used for the infectious particle.

Prion diseases have more recently been identified as protein misfolding diseases. They are acquired either iatrogenically or by ingesting misfolded Prions (PrP^{SC}) among the same species. Kuru occurred after the Fore people of Papua New Guinea would consume the brains of the deceased in a religious ceremony[11]. Occasionally prions can be infectious across species. Although rare, humans who have eaten meat from cows with BSE have been diagnosed with variant CJD (vCJD)[12]. This infectious protein has an incubation time of many years, and most people who have eaten the same meat never have any symptoms of vCJD. Not all prion diseases are infectious. FFI is inherited in an autosomal dominant manner[13], but is still considered a prion disease because it involves misfolding and aggregation of the prion protein.

While not necessarily infectious, many proteins show templating behavior and can be recruited to aggregate and adopt the conformation of the aggregate instead of the functional structure. These aggregates are frequently seen in connection with neurodegenerative diseases. Aβ aggregates in the form of amyloid plaques in AD, α-synuclein aggregates into Lewy Bodies in Parkinson's Disease and Lewy Body Dementia[14], and Tau aggregates into neurofibrillary tangles found in AD, Progressive

Supranuclear Palsy (PSP), Chronic Traumatic Encephalopathy (CTE) and more than 20 other diseases, which are collectively known as tauopathies[15,16,17].

1.1.2 Tauopathies

Although all tauopathies contain fibrillar aggregates of Tau, the causes and symptoms of tauopathies are diverse. AD is the most common tauopathy and affects more than 5,000,000 people in the United States[18]. As the population ages, this number will continue to increase causing strain on caregivers, medical professionals, and insurers. Symptoms begin to appear as difficulty learning new things, and progress to memory loss, speech loss, and eventually loss of motor control.

While AD is the most common tauopathy, there are many more which have a variety of symptoms and causes of onset. Difficulty with balance and eye movement are initial clinical symptoms of PSP. This progresses with continually decreased motor function and cognitive decline in typical PSP. Atypical PSP presents with many of the typical PSP symptoms while cognitive decline is not present[19]. Pick's Disease (PiD) affects the frontal lobe and executive function marked with a change in mood and personality. This leads to difficulty with language and eventually an inability to speak at all[15].

Tauopathies can be initiated by several different pathways. Although AD occurs sporadically in most cases, less than 5% of cases are linked to a small number of gene mutations; however, these gene mutations virtually guarantee AD onset late in life[20]. Similarly, PSP and PiD are typically sporadic with a small number of mutations contributing to a genetic factor for disease. Frontotemporal Dementia with Parkinsonism

linked to Chromosome 17 (FTDP17) is a purely genetic disease. CTE is a tauopathy which is initiated by significant or repeated head trauma, recently highlighted in a study of deceased players from the National Football League, as well as high school and college atheletes[21].

Interestingly, Tau tangles and Aβ plaques are also found in nearly all people with Down Syndrome (DS) above the age of forty[22]. For most with DS, Tau aggregates begin showing up in their 30s, with essentially 100% of people with DS over the age of 60 showing Tau tangles and Aβ plaques. Tau is also hyperphosphorylated in DS the same way hyperphosphorylation occurs in AD[23]. The protein aggregates follow a progression identical to AD. However, not all of those with DS have clinically diagnosable AD.

1.2 Tau Protein

1.2.1 Structure and Function

The microtubule associated protein (MAP) Tau is an intrinsically disordered protein that is primarily found in the brain. Tau has between 352 and 441 amino acids (AAs) in its primary sequence. The MAPT gene encodes for Tau and contains 16 exons, three of which are responsible for the six isoforms found in the adult human brain[24,25]. Exons 2 and 3 dictate the inclusion of zero, one, or two N-terminal inserts. Exon 10 determines the presence or absence of the second of four semi-conserved amino acid repeat regions near the C-terminal end of the protein. Tau is frequently classified as three-repeat (3R) or four-repeat (4R) when describing the protein (Figure 1A). Tau's primary function is to bind and stabilize microtubules. This binding occurs at the repeat

regions of the protein[26]. Even when bound to microtubules, the N- and C-terminal ends of the protein still exhibit disordered behavior[27].

The two isoforms of full length Tau used in this research are hTau23, which has a mass of 36,760 Da, and hTau40, which has a mass of 45,850 Da[28]. Truncated Tau has also been used to mimic the aggregation of Tau *in vitro*. Truncated Tau consists of just the repeat regions with the C- and N-terminal ends removed. The lack of the N- and C-terminal ends allows aggregation to occur faster. K18 refers to the 4R truncated Tau, and 3R truncated Tau is K19[29].

In this work, native cysteines have been removed and replaced by serines at positions 291 and 322 in hTau40 and position 322 in 3R isoforms. The cysteines were removed to inhibit dimerization by disulfide bonds in 3R and 4R isoforms, which could cause spontaneous nucleation to occur quicker[30]. Intramolecular disulfide bonding could create compact monomers in 4R Tau making aggregation more difficult[31,32]. When the cysteines are present, it would be necessary to use a reducing agent to prevent disulfide linkages. By mutating the residues to serine, this additional step is not necessary. The isoforms commonly used in this work are the cysteine-less versions of hTau23 (hTau23cl) and hTau40 (hTau40cl).

1.2.2 Tau Protein in Disease

In disease, Tau undergoes aggregation and spreading throughout the brain. There are two phases in protein aggregation. Nucleation occurs when a minimum number of monomers and cofactors interact and allow an initial nucleus to form[33]. Nucleation is the slow step in the process. Tau has an overall positive charge and requires an anionic

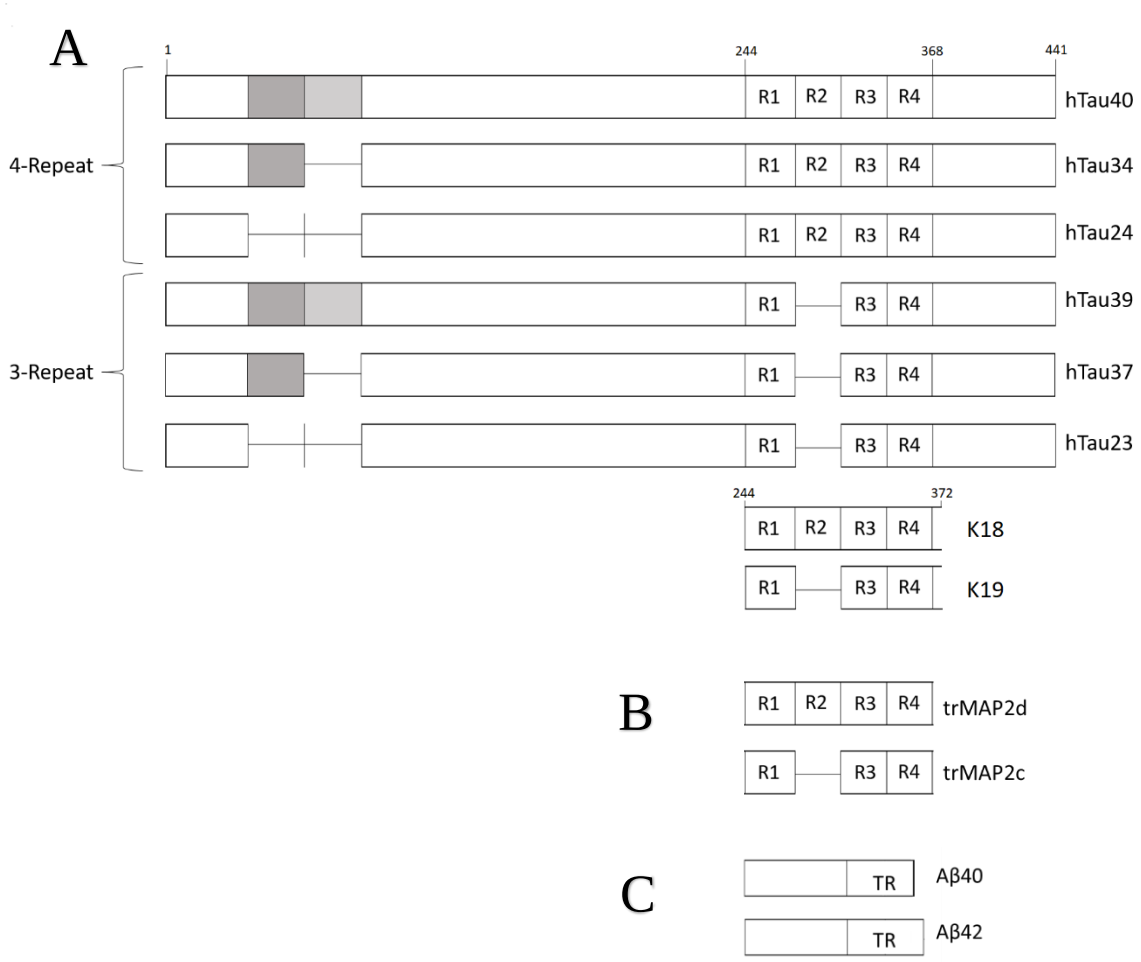

Figure 1: Protein Isoforms. (A) The first three isoforms are the 4R Tau protein isoforms which contain two, one, and zero N-Terminal inserts. Then the 3R isoforms are shown, which also have two, one, or zero N-Terminal inserts. The truncated Tau isoforms K18 and K19, follow. (B) shows the truncated isoforms of MAP2d (4R) and MAP2c (3R). (C) show the proteolytic cleavage products of the two fragments of APP found in disease (Aβ40 and Aβ42) TR refers to the 12 or 14 AA transmembrane region.

cofactor for nucleation to occur. *In vitro*, the polyanionic glycosaminoglycan heparin is frequently used[34]. *In vitro* processes show a long lag phase before nucleation occurs. Once a nucleus is formed, growth can begin. During the elongation phase, monomer adds to the ends of the nucleus to form fibrils of parallel, in-register, cross β-sheets[35,36,37].

1.3 MAP2

MAP2 is a second group of microtubule associated proteins that are also found in the human brain[38]. Like Tau, MAP2 binds and stabilizes microtubules[39]. MAP2c and MAP2d are the shorter isoforms of MAP2 and contain either three (MAP2c) or four (MAP2d) microtubule binding repeats[40]. The MAP2 gene contains 19 exons and is responsible for the expression of each of the isoforms of MAP2[41]. Notably, alternative splicing of exon 7 differentiates between MAP2c and MAP2d. Like Tau, the MAP2 proteins are intrinsically disordered, and in this work truncated forms of MAP2c and MAP2d have been used consisting of only the binding repeat regions. These constructs will be referred to as trMAP2c, which has a molecular mass of approximately 11 kDa and trMAP2d which has a mass of about 14 kDa (Figure 1B).

1.4 Amyloid-β

In addition to Tau, the 40 to 42 AA protein fragment Aβ (Aβ40 or Aβ42) also aggregates in AD forming amyloid plaques (Figure 1C). These amyloid plaques are extracellular aggregates. Aβ is a proteolytic fragment of the Amyloid Precursor Protein (APP) caused by proteolytic cleavage by β-secretase at residue 671 and γ-secretase on the C-terminal end[42]. APP is a transmembrane protein and the Aβ fragment consists of the 28

residues just before the transmembrane region and the first 12 or 14 AAs inside the transmembrane region. This work uses Aβ42, which has a molecular mass of 4.5 kDa.

1.5 Tauopathy Pathology and Diagnosis

1.5.1 Classification of Tauopathies

Tauopathies can be classified by the make-up of the fibrils found in diseased tissue. Three-repeat tauopathies contain fibrils made up of the three 3R isoforms of Tau. The diseases that fall under this category include frontotemporal dementias such as PiD[43]. PSP and CBD are examples of four-repeat tauopathies, which contain only the 4R isoforms of Tau[44]. Diseases like AD and CTE are mixed fibril tauopathies[37]. The aggregates of mixed fibril tauopathies contain all six isoforms.

1.5.2 Pathology

AD Pathology. In AD, Tau is not the only protein to aggregate, but Tau follows a much more predictable course than Aβ. Tau aggregates begin to form in the locus coeruleus and transentorhinal cortex, slowly spreading to the hippocampus and the neocortex[45]. The spread of Tau aggregates closely correlates with mental decline, this is not true for Aβ[46]. AD can be assessed based on the Braak Stage of the spreading of Tau. In stages I and II, the tangles are relatively few and only in the cerebral cortex. No symptoms are present. In stages III and IV, NFTs have spread to the hippocampus and some memory loss has occurred. By stages V and VI, aggregates are seen throughout the brain tissue and clinical diagnosis is possible. NFTs in AD contain all six isoforms of Tau[23], and individual synthetic fibrils have been shown to contain both 3R and 4R Tau[37]. Gradual cognitive decline is the primary outward symptom of this disease.

Misfolded Tau has been shown to propagate between neurons and recruit endogenous Tau proteins onto their ends[47]. While the mechanism is not fully understood, direct protein to protein interactions have been suggested[48]. The intercellular spread of Tau pathology has been suggested as the primary mechanism of aggregation, and synaptic transmission appears to be the most likely culprit[49]. Recent research has suggested that an increase in synaptic activity can lead to faster spreading of aggregates[50].

PSP Pathology. The brain tissue of people with PSP only contains fibrils of 4R Tau[44]. Symptoms include unsteadiness and a drifting gaze and in some instances, mental decline occurs[19]. Pathologically, these Tau aggregates start in the subcortex and for patients with no dementia, the aggregates mostly remain in that area[51]. Those who do have mental decline along with PSP show some aggregates in the cerebral cortex, consisting of Braak Stage I and II as seen in AD. Much less common in PSP are Braak Stages of III through VI.

Clinical Diagnosis. Clinical diagnosis of tauopathies is achieved by various physical exams, psychological exams, and caregiver or self-assessments. This frequently leads to misdiagnosis among tauopathies. For example, CBD can be clinically diagnosed as PSP as much as 50% of the time[51]. Currently, the only way to confirm the diagnosis of a tauopathy is by looking at brain pathology at autopsy.

1.5.3 Current Detection Methods

Antibodies. Currently, there are several ways to detect the presence of Tau in tissue, but there are problems with these methods. Antibodies exist to detect different forms of Tau in tissue. These include “whole Tau” or all isoforms of Tau[52], Tau with

specific phosphorylation sites[53,54], and Tau with specific truncation sites[55], among other posttranslational modifications. These antibodies can be used in assays including ELISA, Western Blotting, and immunohistochemistry. The methods require a relatively small amount of tissue. However, the problem with many antibodies is that monomers and fibrils cannot be differentiated.

Amyloid Sensitive Dyes. Certain dyes have been shown to differentiate between fibrils and monomer *in vitro*. These dyes can also be used to detect amyloid-like protein aggregation *in vivo*. Congo Red (CR) is a dye used since the 1920s to detect amyloids in brain tissue[56]. A more recently discovered dye, Thioflavin T (ThT) is much brighter and more sensitive than CR[57]. The structures of ThT respond to the β-sheet structure present in amyloids, but ThT does not differentiate between various proteins[58]. Prion, α-syn, and Tau aggregates all respond to amyloid dyes in a similar manner. The dyes also require a larger amount of Tau fibrils than are required for antibodies in order to be identified.

1.6 Cofactors

Polyanionic cofactors such as heparin, described above are required for aggregation of Tau[59]. Other known cofactors include single and double stranded RNA and Poly Glutamate, each also polyanionic[60]. It has been shown that each of these potential cofactors allow for aggregation *in vitro* and can be used in various aggregation assays. Heparin is a long chain sugar with each of the sulfate arms measuring approximately 5.7 Å from one another[61]. The measurement between the phosphate groups in single stranded RNA is 3.4 Å[62]. The same measurement holds for the double stranded RNA PolyA/U, however single stranded RNA can have more complicated tertiary structure while double

stranded RNA forms a double helix due to the interaction of the base pairs with one another[63]. Poly Glutamate is a peptide with the side chains carrying the negative charges. Due to flexibility of the side chains, the distance between negative charges can change depending upon the folding of the peptide. Given that the distance between Tau monomers in fibrils is about 4.7 Å[35], cofactors could interact with aggregates in different ways.

Polyamines, which have an overall positive charge could have a place in aggregation as well. Tau has an overall positive charge, but contains both negatively and positively charged residues throughout. It is possible that the positive charges on the polyamines can interact with the negatively charged AAs in the sequence and stabilize the structure allowing nucleation and growth to occur. In this work the polyamines used were small molecules with between two and four amines on a carbon backbone (Figure 2). Agmatine contains two primary amines and a secondary amine at the first carbon and a primary amine on the fifth carbon. Putrescine is a four-carbon chain with a primary amine on the first and fourth carbon. Spermidine has three amines including a primary amine at carbon one, a secondary amine between carbon three and four, and a primary amine at carbon seven. Spermine is the longest polyamine with primary amines at carbons one and ten and secondary amines between carbons three and four as well as carbons seven and eight.

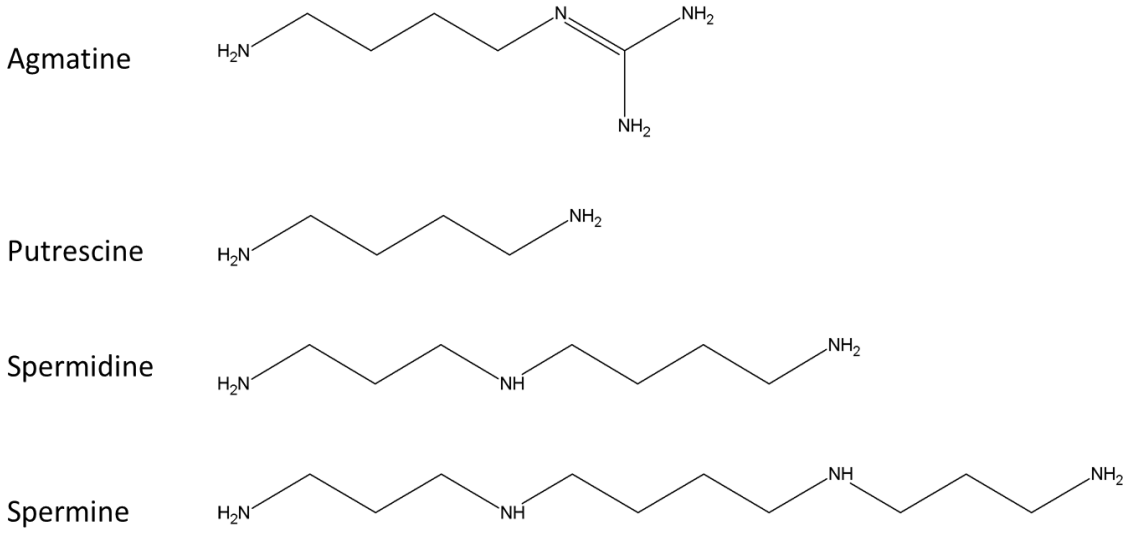

Figure 2: Polyamines. The polyamines were used as potential cofactors for Tau and Aβ aggregation. Their single bond structure allows polyamines to rotate freely and adapt to the length most beneficial to aggregates.

1.7 Amplification Assay

1.7.1 Prion Amplification

Within the prion field, an assay to detect PrP^{SC} was developed by Soto *et al*[64]. This procedure combined extract from PrP^{SC} hamster brains with healthy hamster brain extract, as a source of natively folded PrP. The solution is then subjected to several rounds of sonication and incubation. Incubation allows PrP to add itself to the ends of the PrP^{SC} in brain tissue extract (Figure 3). Sonication breaks the existing aggregates in the brain extract offering more ends for PrP from the undiseased extract to add on to. In the case of PrP, this assay is sensitive enough to detect PrP^{SC} in pre-symptomatic animals including hamsters and cattle[65].

1.7.2 Application of Assay to Tau Amplification

The PrP^{SC} assay described above has been adapted to detect minute amounts of Tau fibrils from human brain extract. This assay relies on the addition of approximately 4% by volume of homogenized brain extract to recombinant Tau monomer. Repetition of cycles of sonication and incubation cause amplification of a lower quantity of seeds in a much faster manner than had previously been accomplished[66]. When developing this amplification assay a negative control was required. In this assay, an unseeded control was maintained to ensure that spontaneous nucleation did not occur.

Various conditions of the experiments were adjusted to suppress nucleation, while still allowing growth. The prion field also introduced another amplification assay with what it titled “Real-Time Quaking Induced Conversion” or RTQuIC[67]. In this assay, cycles of vigorous shaking followed by resting replace the sonication/incubation scheme.

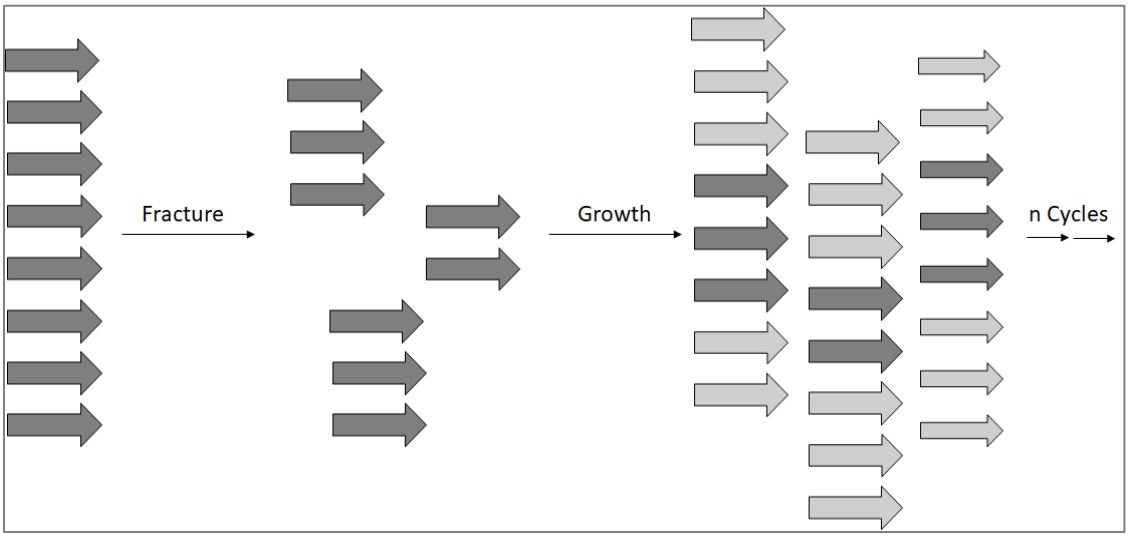

Figure 3: Amplification Schematic. The above figure shows the amplification process. Starting with one fibril, the fracture step breaks it up into several shorter fibrils while the growth step allows monomer in solution to grow onto the shorter fibrils. This is repeated over n-cycles causing amplification

These cycles cause faster growth of PrP^{SC} and could possibly be adapted for use with Tau to detect aggregates in biological samples. Because both nucleation and growth occur earlier[67], the shaking assay may decrease experimental time and allow for faster results. Environmental conditions were also investigated. NaCl concentrations were altered to see how electrostatic interactions would influence nucleation and/or growth of Tau. High salt concentrations would increase the amount of positive and negative charges in solution, possibly interfering with the positive charge on Tau and negative charge of Heparin, decreasing the likelihood of nucleation[68]. Heparin was replaced with various cofactors to determine if a structurally unique cofactor would have an effect on nucleation and/or growth.

1.7.3 Thesis Objective

The following work outlines the steps that have been taken to develop an amplification assay with the sensitivity to detect fibrils from biological samples. Improvement to the sensitivity and specificity for various biological samples is sought and applications of the assay's capability are demonstrated. Future application and development of this assay could lead to detection of Tau fibrils in blood samples leading to earlier diagnosis and treatment of AD and other tauopathies.

Chapter Two: Methods

2.1 Transformation

Between 100 pg and 1 ng of the plasmid of interest was combined with 20 μL BL21(DE3) competent *Escherichia coli* (*E. coli*) cells (Agilent) and incubated on ice for 30 min, followed by heat shock for 30 s at 42°C and recovery on ice for 2 min. One mL of NZY medium (10 g/L NZ-amine, 12.5 mM $MgSO_4$, 12.5 mM $MgCl_2$, and 20 mM glucose) was added and mixture was then incubated while shaking at 37°C for 1 hour. Cells were plated on a Luria-Bertani (LB) broth (Difco) agar plate with 20 mg/L kanamycin (Gold Biotechnologies) and incubated at 37°C overnight. A single colony was selected and combined with LB Miller broth at a concentration of 20 mg/L with kanamycin at a final concentration of 140 μM. Culture was incubated at 37° overnight and a glycerol stock was created by combining culture and sterile glycerol in a 1:1 ratio. The glycerol stock was stored at -80°C.

2.2 Expression

For protein expression, overnight cultures were made using glycerol stocks of transformed BL21(DE3) competent cells in LB broth at a concentration of 20 mg/L with kanamycin at a final concentration of 140 μM. Cultures were incubated at 37°C for 17 hours. The overnight culture was added to LB broth and kanamycin in a ratio of 1:100 and incubated at 37°C until the optical density at 600 nm (OD600) reached 0.75-1.00.

Upon reaching the optimal OD600 expression was induced using isopropyl β-D-1-thiogalactopyranoside (IPTG, Gold Biotechnologies) at a final concentration of 1mM and incubated for an additional 3.5 to 4 hours. Cells were centrifuged at 4000 x g for ten minutes and resuspended in a buffer containing 20 mM piperazine-N,N'-bis(2-ethanesulfonic acid) (PIPES, J.T. Baker), 500 mM Sodium Chloride (NaCl, Fisher Scientific) and 5 mM ethylenediaminetetraacetic acid (EDTA, J.T. Baker) and frozen at -80°C until purification steps.

2.3 Purification

2.3.1 Purification of Full Length Tau

Ion Exchange Chromatography Following expression, the bacterial suspension was heated in a water bath at 80°C for 30 minutes and transferred to an ice bath for 5 minutes. Samples were then sonicated with a probe sonicator (Thermo-Fisher) for one minute at 50% amplitude and centrifuged at 15,000 x g for 30 minutes. Fifty-five percent weight/volume ammonium sulfate (MP Biomedicals, LLC) was added to the supernatant and shaken at room temperature for not less than one hour. After the salt was completely dissolved, the solution was centrifuged for ten minutes at 15,000 x g, the supernatant was decanted and the pellets were centrifuged again with the same settings. The pellets, with all supernatant carefully removed were resuspended in nanopure water with 2mM dithiothreitol (DTT, Gold Biotechnologies) and sonicated for one minute at 50% amplitude. The solution was then filtered using a 0.45 μm Acrodisc GxF/GHP membrane filter (Pall Life Sciences). The sample was then loaded on to a Mono S 10/100 GL cation exchange column (GE Healthcare). Protein was eluted via a linear salt gradient (50−1000

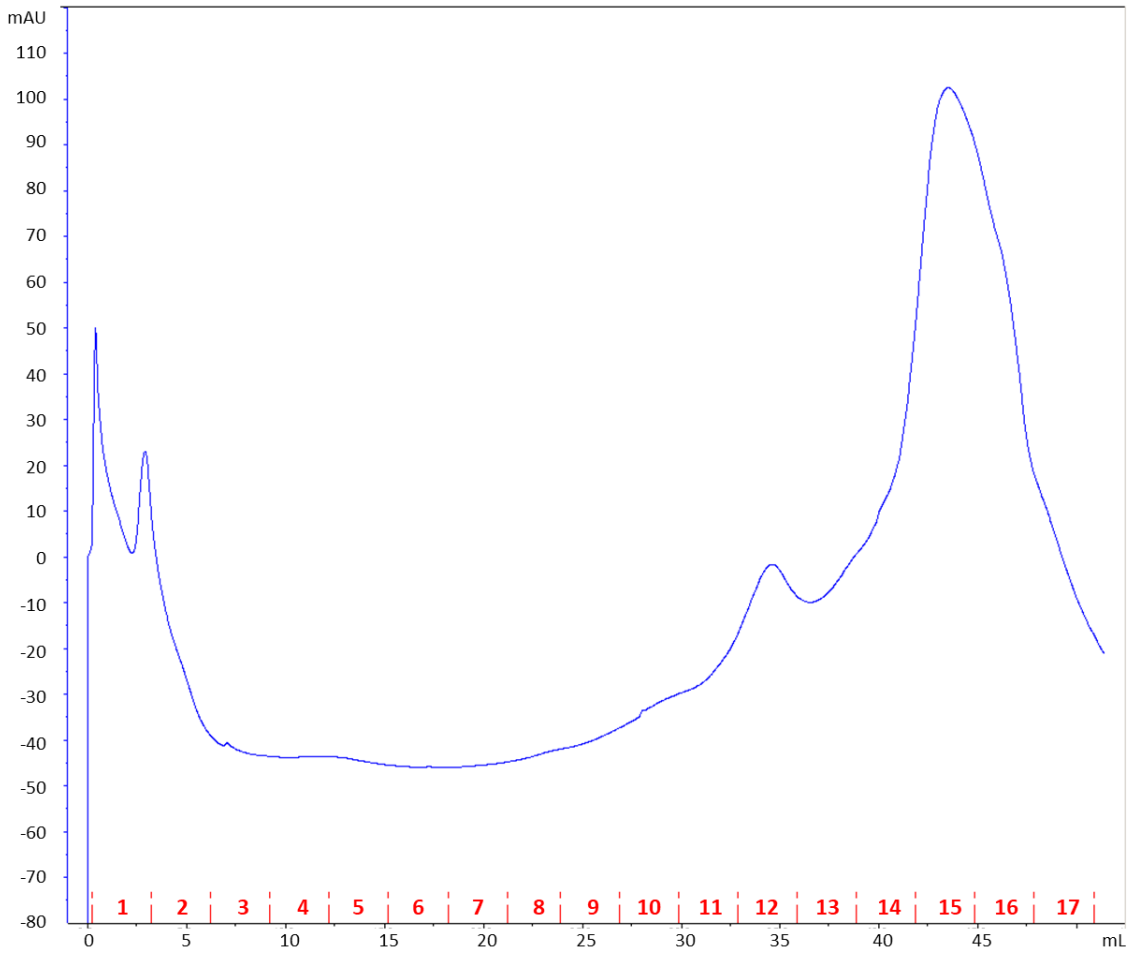

Figure 4: Cation Exchange Chromatography Output. Following the UV trace at 280 nm the peak can be seen between fractions 11-17. These are the fractions that were chosen to run on an SDS-PAGE gel (figure 5).

mM NaCl, 20 mM PIPES, pH 6.5, 2 mM DTT). Fractions 11 through 17 were collected as determined by figure 4 and run on SDS-PAGE (figure 5) to determine the fractions with the highest concentration of protein.

SDS-PAGE. SDS-PAGE gels were prepared with a 4% bis-acrylamide stacking gel and a 12% bis-acrylamide separating gel. Running buffer containing 25 mM Tris Base, 190 mM Glycine and 0.1% SDS was added to the gel cassettes and the running box. Samples were added to dilute the 4x sample buffer with 40% sucrose, 240 mM Tris, pH 6.8, 8% SDS, and 0.1% bromophenol blue to 1x and 6 μL were loaded into each well. Gels were run at 20 mA per gel for approximately 50 min, or until the blue running front was at the bottom of the gel. Gels were stained with 0.1% Coomassie brilliant blue R250 (ThermoFisher), 50% methanol (ThermoFisher) and 10% glacial acetic acid (ThermoFisher) for one hour and destained in solution made with 40% methanol and 10% glacial acetic acid for 1 hour. Gels were imaged using the Epson Scan V750 PRO. As seen in figure 5, the fractions chosen would have been 14, 15 and 16.

Size Exclusion Chromatography. After cation exchange, size exclusion chromatography was performed. A buffer containing 20 mM Tris pH 7.4, 1 mM EDTA and 100 mM NaCl was used to run samples over a Superdex 200 gel filtration column (GE Healthcare). As seen in figure 6, fractions 57 through 61 were collected and 50% volume/volume methanol (Fisher Scientific) was added along with 2 mM DTT and stored on ice overnight. Precipitated protein was centrifuged at 15,000 x g for 10 minutes, the supernatant was removed and 1 mL of supernatant was used to transfer the precipitate into a smaller tube. The suspension was centrifuged at 11,000 x g for 10 minutes, and the

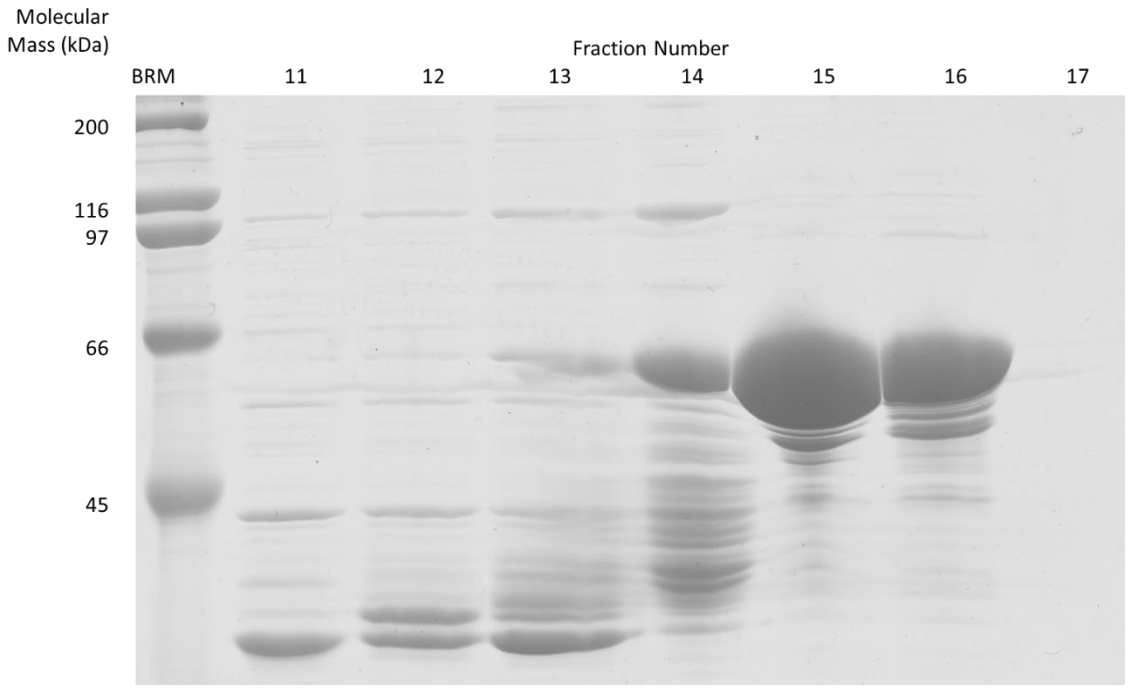

Figure 5: Ion Exchange Gel. This 12% SDS-PAGE gel stained with Coomassie blue stain demonstrates fractions 11-17 from one sample of cation exchange chromatography. The fractions selected for further purification of hTau40cl would be 14, 15 and 16.

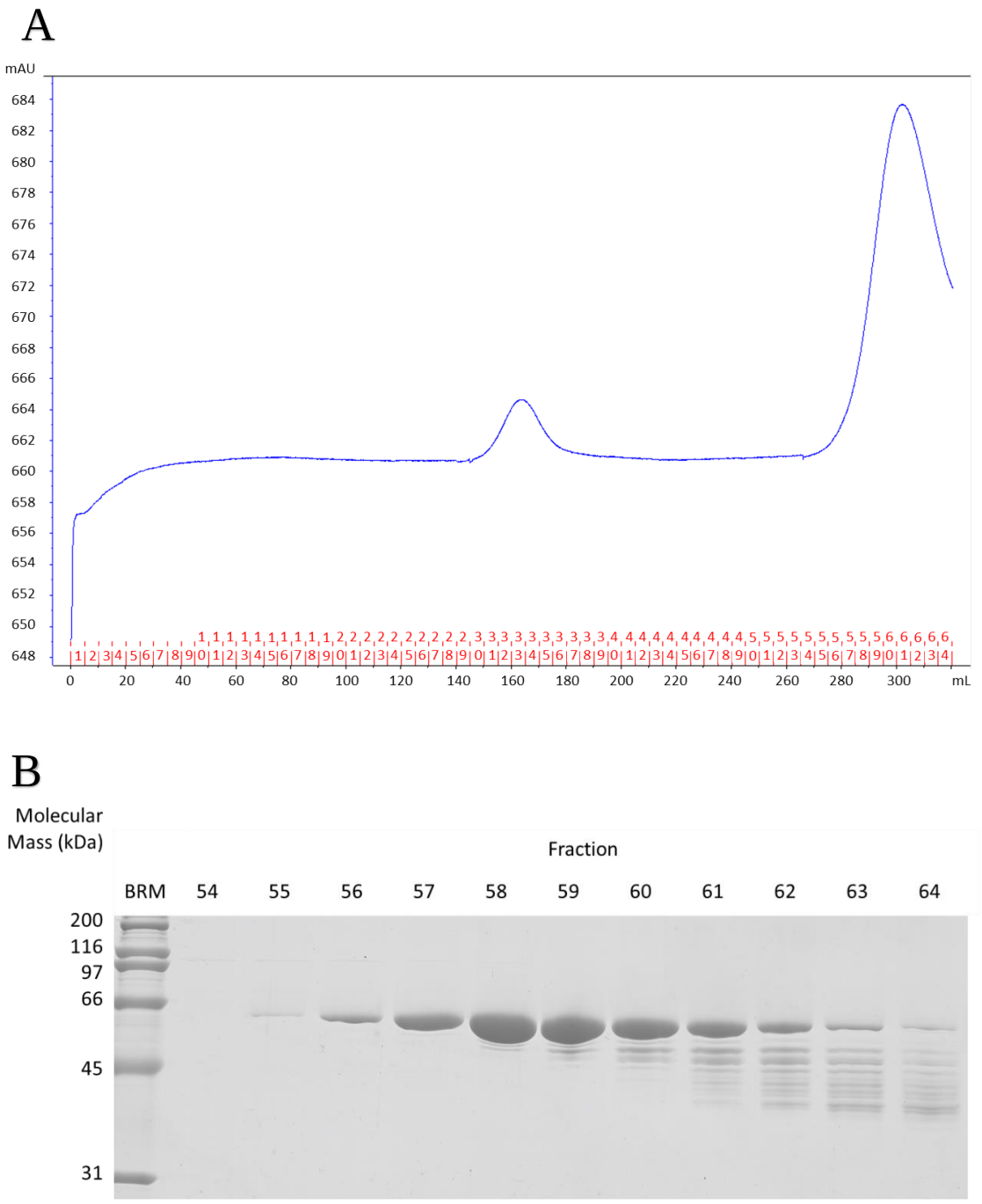

Figure 6: Size Exclusion Chromatography Output. (A) The dark blue line shows the absorbance at 280 nm for the sample that was run over the size exclusion column. (B) Fractions 54-64 were chosen for a 12% SDS-PAGE gel stained with Coomassie blue Stain to asses purity. Fractions 57-61 were selected.

supernatant was removed and replaced with 1 mL methanol with 2 mM DTT. The pellet was washed with methanol and stored at -80°C until needed.

To monomerize the protein, methanol was removed from the pellet and 8 M Guanadine Hydrochloride (GdnHCl, ThermoScientific) was added to dissolve the pellet. Two or three pellets were combined resulting in 200 μL pellet dilutions. The 200 μL were added to a PD-10 column (GE Healthcare) followed by 1.8 mL of assembly buffer containing 10 mM HEPES, pH 7.4, 100 mM NaCl, 0.5 mM EDTA and 0.1 mM sodium azide (NaN_3). An additional 2.0 mL of assembly buffer was added to the column and collected. Protein was quantified via the bicinchoninic acid (BCA) assay (ThermoScientific).

2.3.2 Purification of Truncated MAP2

Truncated MAP2 was expressed and purified by a coworker in the laboratory identically to full length Tau with the following exceptions: Before cation exchange chromatography, the filtered protein solution was diluted with 2 M Urea (Fisher Scientific) and eluted in later fractions. Fifteen percent bis-acrylamide gels were used to determine the purity of the truncated protein upon completion of cation exchange chromatography. After size exclusion chromatography, selected fractions were split in three equal amounts and a four-fold excess of acetone was added, along with 2 mM DTT. MAP2 pellets were stored in acetone until monomerized.

2.4 Amplification Assay

2.4.1 Preparation of Seeds

Recombinant Seeds. Seeds for hTau23cl and hTau40cl were created using 25 μM Tau and 12.5 μM heparin. Buffer containing 100 mM NaCl, 10 mM HEPES, pH 7.4 was added for a total volume of 500 μL. An Eppendorf Thermomixer R with 1.5 mL tube holder attachment was used to shake seeds at 1,000 RPM at 37°C with one minute cycles consisting of 30 s shaking and 30 s resting. Seeds were created using these settings for 48 hours unless otherwise stated.

Tissue Homogenate Seeds. Brain tissue from the cerebral cortex, provided by University of California Alzheimer's Disease Research Center and Medical University of South Carolina Brain Bank, Carroll A. Campbell, Jr. Neuropathology Laboratory, was combined with a buffer containing 10 mM HEPES at pH 7.4, 5 mM EDTA, 150 mM NaCl, 0.1% Triton X-100 and Halt Protease Inhibitor (Thermo Scientific) in a 1:10 weight/volume ratio. The mixture was homogenized on ice in a Potter-Elvehjiem tissue grinder (Wheaton) at 250 rpm using SteadyStir Digital (Fisher Scientific) for 5 minutes, followed by centrifugation for 20 minutes at 5,500 x g at 4°C. The BCA assay was performed on a 1:10 dilution of the supernatant to gain an approximate total protein concentration. The supernatant was then aliquoted, flash frozen and stored at -80°C until needed.

2.4.3 Amplification of Synthetic Tau Fibrils.

Sonication cycles (the number of cycles depended on experiment and is specified in the Results section) were achieved using a bath sonicator in which a water-filled

microplate horn was coupled to an ultrasonic processor (QSonica). A single cycle consisted of 5 s sonication pulses at 5% amplitude. The water temperature was held constant at 37 °C using a recirculating chiller for the incubation cycles, which were 30 min. The reactions were contained within Nunclon 96-well plates (Thermo Scientific) and were covered with BioDot Microplate sealing tape (Dot Scientific). Each well in the microplate corresponded to an individual experiment. Thioflavin T (ThT, Sigma), when appropriate, was used as the fluorescent indicator of fibril growth. The following were added to each well: 10 μM Tau monomer (htau40 or htau23), 40 μM heparin (Celsus, average MW ≈ 5000), 5 μM ThT (when appropriate), indicated concentration of seeds, and additional buffer (100 mM NaCl, 10 mM HEPES, pH 7.4) to make the total sample volume 200 μL.

In some experiments, heparin was replaced with other anionic cofactors. These include the single strand RNAs PolyA and PolyU (Sigma Aldrich), the double strand RNA PolyA/U (Sigma Aldrich) and poly-glutamate (Sigma Aldrich). These alternative cofactors were substituted at a concentration of 50 μg/mL. Various polyamines (Sigma Aldrich) were also used as cofactors in the concentrations provided in the results section. Some experiments were performed with NaCl concentrations other than 100 mM. Results will indicate when a different concentration of NaCl is used.

Control wells were run alongside each experiment. A monomer control contained all components except seeds to show that aggregation in the reaction wells occurred through amplification, not through spontaneous nucleation. All microplate experiments involved diluting the initial seeds which were added to reactions prior to incubation or

sonication cycling and were present according to the molar percentage of seed per monomeric Tau, 10 μM for all experiments.

Buoyant bulbs were attached to either side of the microplates to prevent sinking into the sonicator bath. Following amplification, the plate was centrifuged at 1650 x g for 2 min to remove condensation from the sealing tape. If ThT was added, fluorescence was immediately measured using a Tecan Infinite M1000 microplate reader. ThT was excited at 440 nm, and spectra were collected by scanning emission at 480 nm. The Z position of the plate within the reader was kept constant. Tau aggregation was determined by ThT emission at 480 nm.

In addition to ThT as a fluorescent readout, fibrils were sedimented and analyzed on an SDS-PAGE gel with Coomassie staining to monitor amplification over successive cycles. Experiments were performed by preparing three microplate wells with the same components. Following ThT measurement, these wells were pooled and centrifuged at 100,000 x g for 30 min at 10°C. Pellets were dissolved in indicated concentration of 1× SDS-PAGE sample buffer, and run on a corresponding gel.

2.4.4 Amplification of Tau Fibrils from Brain Homogenate.

Experimental parameters were altered for use on brain tissue to account for interference from extracellular components. Reactions were carried out with 10 μM hTau40cl or hTau23cl and 40 μM heparin in buffer (100 mM NaCL, 10 mM HEPES, pH 7.4). Brain tissue homogenate was prepared for amplification as described above. The homogenate was then sonified in the bath sonicator at 10% amplitude for 60 s. A total weight of 20 μg of brain tissue extract (protein mass) was added to each 200 μL final

reaction volume. Using the same power settings as those with recombinant material, 30 cycles of sonication and incubation were performed.

2.4.5 Blockage Using Seeds from AD Extract.

Blockage reactions using brain homogenate were carried out with 10 μM htau40, 40 μM heparin, 0.5 mM Tris(2-Carboxyethyl)phosphine Hydrochloride (TCEP, Gold Biotechnology) and either 10 μM trMAP2c or 5 μM trMAP2d in buffer (100 mM NaCl, 0.1 mM NaN_3, 10 mM HEPES, pH 7.4). Brain tissue homogenate was prepared for amplification by sonication in a bath sonicator with a water-filled microplate horn coupled to an ultrasonic processor at 10% amplitude for 60 s. A total weight of 30 μg of brain tissue extract was added to each 200 μL final reaction volume and 30 cycles of sonication and incubation were performed as described above.

Controls were run alongside each experiment. The positive control consisted of all components except trMAP2 being added to the wells to show standard amplification of AD extract. The negative control consisted of undiseased, tangle-free control extract replacing AD extract in the presence of Tau and heparin, displaying that no growth occurred. Each 200 μL experiment was run in triplicate and combined to be centrifuged for 30 minutes at 100,000 x g. The supernatant was removed and the pellet taken up in 100 μL 1x sample buffer and run on an SDS-PAGE gel with Coomassie staining. Gels were then analyzed using ImageJ software and plotted in GraphPad.

2.5 Seeded Reactions

Seeds, either recombinant and formed as described above or the product of amplification from diseased tissue, were used in seeded reactions. All seeds were

sonicated with a probe sonicator (Thermo-Fisher) for 30 seconds at 20% amplitude prior to the dilution. The following were added to each well of a 96 well plate: 10 μM Tau monomer (hTau40cl or hTau23cl), 40 μM heparin (Celsus, average MW = 5000), 5 μM ThT (when appropriate), indicated concentration of seeds, and additional buffer (100 mM NaCl, 10 mM HEPES, pH 7.4) to a final volume of 200 μL. These plates were incubated at 37°C for the time indicated. If ThT was added, the reaction was monitored in a FLUOstar Omega (BMG Labtech) at 37°C with excitation at 440 nm and emission at 480 nm for the indicated length of time.

2.6 Negative Stain Transmission Electron Microscopy

200-mesh carbon-coated copper grids were placed for 1 min onto 10 μL drops of sample (10 μM of fibrils based on monomer concentration) and then for 30 s onto 10 μL drops of 2% uranyl acetate. The grids were air-dried on filter paper. Images were taken with a Philips/FEI Tecnai-12 electron transmission microscope at 80 keV, equipped with a Gatan CCD camera. Electron microscopy for trMAP2 blockage experiments was performed by Michael Holden.

2.7 Shaking Assay

Monitoring for spontaneous nucleation occurred by using the same concentrations of Tau and heparin (or other cofactors) that were used in the sonication and incubation amplification assay. The shaking and resting cycles were varied as mentioned in the results, as were the speed of shaking and the temperature of incubation. To determine nucleation, two different methods were used. Initially, using the Thermomixer R, after a set amount of time, the reactions were centrifuged at 100,000 x g for 30 minutes. The

pellets were dissolved in an equivalent amount of 1x sample buffer as total supernatant. Pellets and supernatants were then run on an SDS-PAGE gel. The protein that shows up in the pellet implies nucleation. Any protein left in the supernatant has not yet been added to the aggregates, which suggests that it is still monomeric.

Alternatively, nucleation could be monitored in real time using the FLUOstar Omega (BMG Labtech). Aggregation was monitored by adding ThT to the reaction described above at a concentration of 10 μM. Shaking occurred at varying times, RPMs, and temperatures. Excitation occurred at 440 nm and emission was read at 480 nm. Data points were taken every two minutes. This method was used for monitoring the aggregation of Tau as well as Aβ42 which was purchased from Bachem.

2.8 Proteolysis

Proteolysis was performed with the enzyme Proteinase K (PK). Fibrils were grown on 5% seeds taken after amplification. The final concentration of 25 μM Tau, and 12.5 μM heparin was incubated at 37°C for 16 hours. Following the incubation, a portion of the fibrils were centrifuged at 100,000 x g for 30 minutes at 10°C. A BCA assay was run on the supernatant to determine the concentration of fibril monomer equivalents (ME) in the solution. A dilution of AD and PSP derived fibrils was made so that each of the solutions had a final concentration of 10 μM hTau40. The indicated concentration of PK was added to fibrils grown from seeds derived from AD and PSP tissue and allowed to incubate at room temperature for 30 minutes. To end the proteolysis, a final concentration of 4 mM phenylmethane sulfonyl fluoride (PMSF, Sigma) was added to the solution. The

reactions were immediately run on an SDS-PAGE gel with Coomassie staining for analysis.

2.9 Analysis of SDS-PAGE Gel by ImageJ

SDS-PAGE gels were analyzed using ImageJ freeware (National Institutes of Health, USA, public domain). Previously scanned gels were opened in ImageJ and the rectangular selection tool was used to select the first lane followed by selecting "Analyze", "Gels", "Select First Lane". The first rectangle drawn was dragged to the next lane followed by selecting "Analyze", "Gels", "Select Next Lane" for as many additional lanes as were needed. With lanes chosen, "Analyze", "Gels", "Plot Lanes" were selected. This provided density line plot with higher values corresponding to more band density. A line was drawn across the bottom of the desired peak to separate that peak from the background of the gel. The wand (tracing) tool was then selected and used to click under the selected peaks which provided an area under the curve in number of pixels. The areas were transferred to Excel (Microsoft) and percentage growth was calculated by using the total of the pellet and supernatant areas to divide the area of the pellet and multiplied by 100.

Chapter Three: Results

3.1 Recombinant Seeds are Amplified Using Sonication/Incubation Cycles

Cycles of sonication and incubation have been shown to allow for amplification of Tau fibrils from AD brain extract, and no amplification is shown from undiseased control brain extract[66]. When recombinant full-length Tau is incubated at 37°C in the presence of decreasing amounts of seeds for 15 hr, the limit of detection can be determined. Without repeated sonication steps, that limit is 500 nM ME seeds for hTau23cl and 100 nM ME seeds for hTau40cl (figure 7). In order to improve upon this limit, 30 cycles of 5 s sonication followed by 30 min incubation for a total experimental time of 15 hours was introduced. With repeated sonication, the limit is reduced to 10 pM seeds in both hTau23cl and hTau40 (figure 7).

3.2 Tau Fibrils Are Amplified from Diseased Tissue

3.2. 1 Brain Tissue Background

One of the greatest strengths of repeated cycles of sonication and incubation is the ability to amplify protein aggregates from biological samples[66]. Prior to amplification, brain tissue was homogenized and analyzed for protein content. Tangle free control tissue, as well as diseased tissues with pathologically diagnosed tauopathies were compared using SDS-PAGE. Figure 8 shows that each of the different homogenized

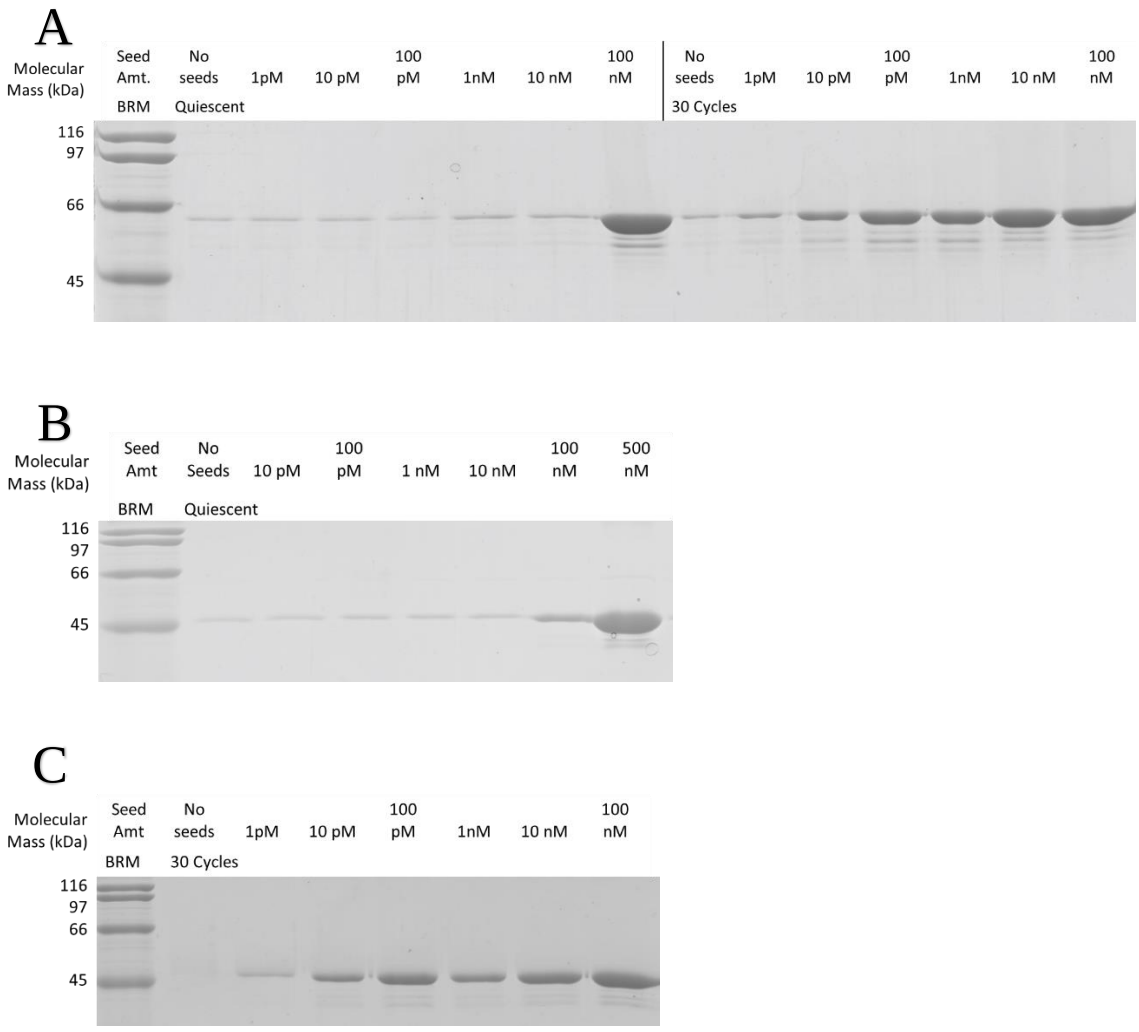

Figure 7: Quiescent vs. Amplified Seeded Reactions. (A) When a dilution series of recombinant hTau40cl seeds are offered to 10 μM hTau40cl monomer and incubated quiescently for 15 hours growth is not detected until 100 nM ME seeds are provided. When an identical solution of hTau40cl monomer and seeds are subjected to 30 cycles of sonication and incubation, for a total experiment time of 15 hours, growth can be seen with as few as 10 pM ME seeds. (B) During 15 hours of quiescent growth, hTau23cl begins to show growth at 100 nM ME seeds, but only at 500 nM can strong growth be seen. (C) After 30 cycles of sonication and incubation, growth of hTau23cl can be seen with 10 pM ME seeds. All SDS-PAGE gels are 12% bis-acrylamide and stained with Coomassie blue stain.

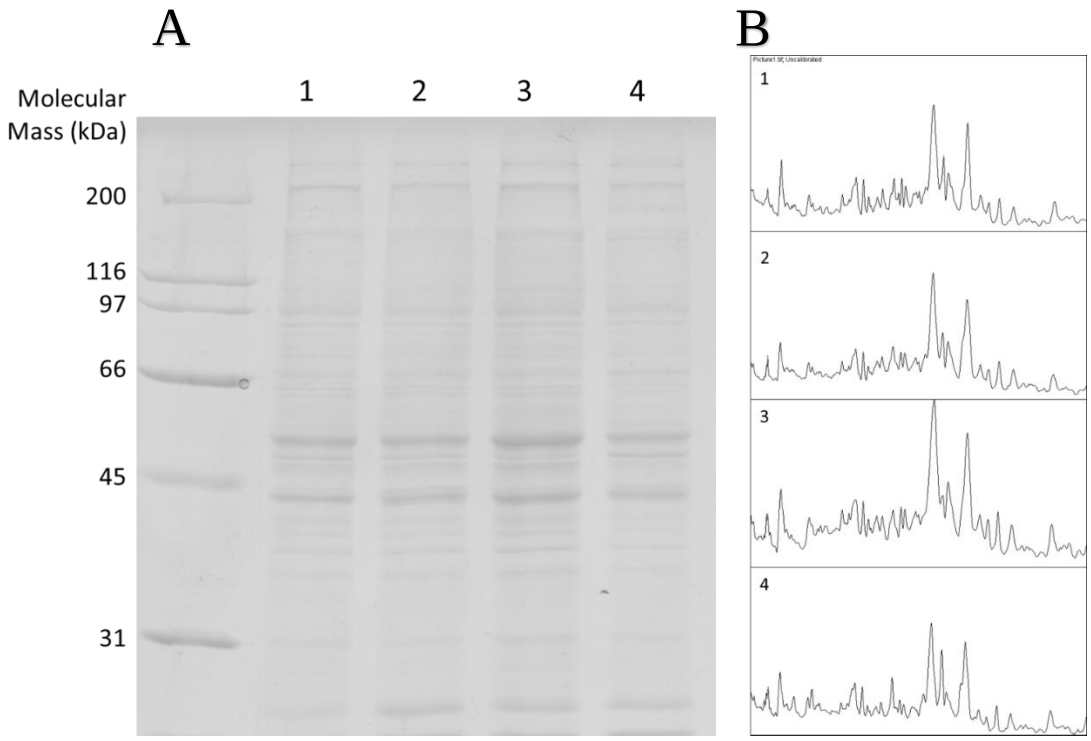

Figure 8: Brain Tissue Background Comparison. (A) shows the SDS-PAGE gel stained with Coomassie blue stain, (B) shows the density analysis of the SDS-PAGE gel from ImageJ. Both show that there are no discernable differences between diseased and undiseased tissue homogenate. Sample 1 is undiseased tissue, 2 is AD, 3 is PiD, and 4 is PSP.

tissues have comparable protein content: there is no observable difference between homogenized tissue from undiseased tissue, AD tissue, PiD tissue, and PSP tissue.

3.2.2 Amplification

To demonstrate amplification of fibrils from extract using Tau protein, AD brain and undiseased brain were homogenized, diluted, and then added to recombinant hTau40cl or hTau23cl. Next, the samples were subjected to 30 cycles of amplification, with each cycle consisting of 5 s of sonication and 30 min of incubation at 37 °C. Only the sample that contained AD extract was able to template growth of both hTau23cl and hTau40cl (Figure 9A). Importantly, spontaneous nucleation could be excluded, as neither hTau40cl nor hTau23cl in the presence of undiseased brain caused aggregation. The fibrillar nature of the amplified protein aggregates was verified by electron microscopy (EM) (Figure 9B and 9C). Combined, the findings indicate that Tau fibrils can be selectively amplified from Tau seeds inherent in the crude AD brain extract.

3.2.3 Variability in Amplification

Identical reactions performed in multiple wells in the microplate displayed varying amounts of amplification. Emission spectra indicate that the variability in amplification can arise, sometimes deviating due to a single reaction. It is possible that this variability originates due to an uneven force distribution in the bath, a finding that was suggested previously[69]. Slight variability was also seen in the power output between experiments using the same bath sonicator and among different bath sonicators.

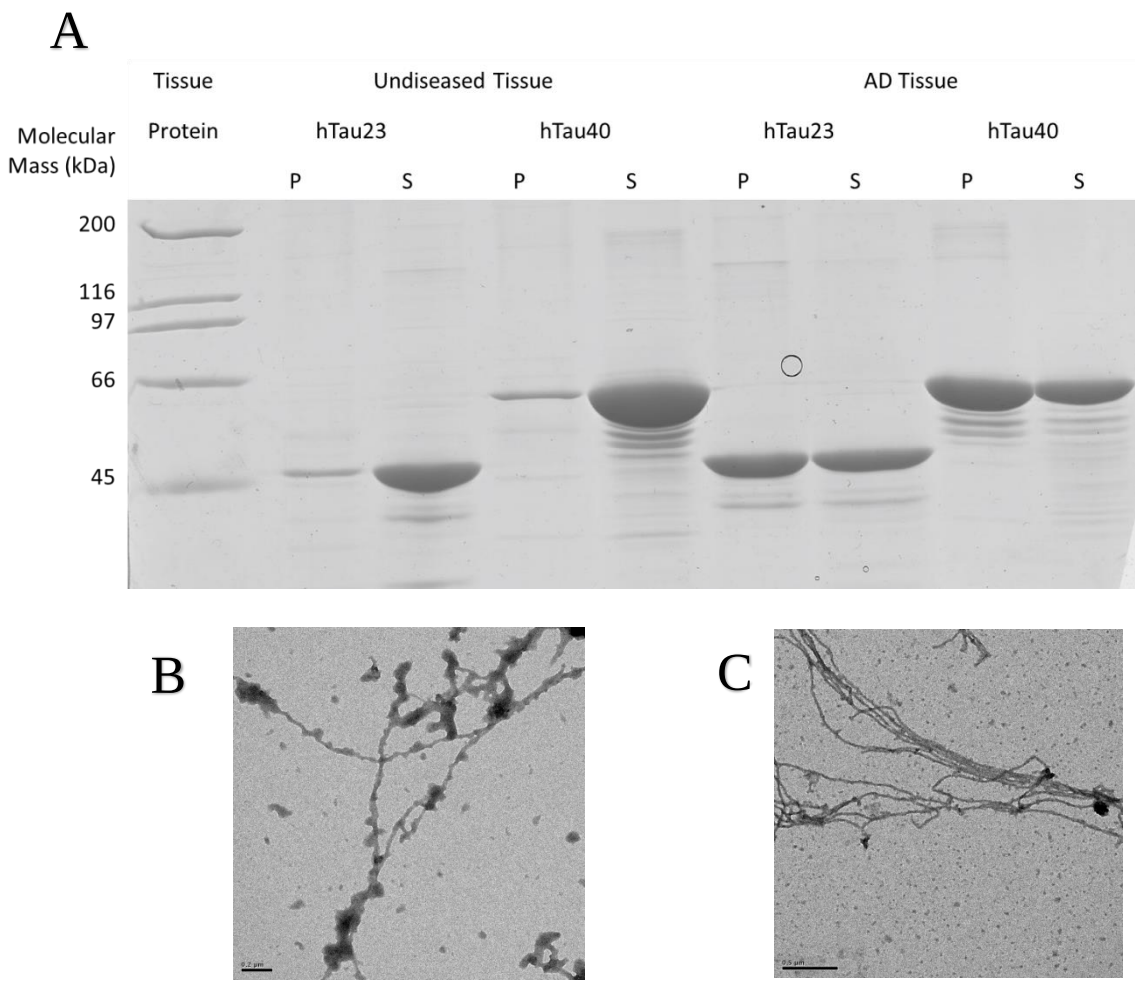

Figure 9: Amplification of Seeds from Brain Tissue. (A) The SDS-PAGE gel with Coomassie blue staining shows that aggregation does not occur when using tissue from undiseased brain using either hTau23cl or hTau40cl, but both grow when in the presence of AD tissue. Wells marked with "p" are pellets after a high-speed centrifugation, Wells marked with "s" are the corresponding supernatants. B show an electron micrograph of hTau23cl amplified from AD extract. Scale bar = 200 nm. C shows hTau40cl amplified from AD tissue. Scale bar = 500 nm.

3.3 Other Factors Affect Nucleation and Growth of Tau

Aggregation of Tau takes place in two basic phases. Nucleation is the required first step for aggregation to occur. This involves the creation of the smallest template which can be used for templating fibril growth, which is the second phase. In order to create a more sensitive assay, conditions were screened to determine which could best suppress nucleation, while still allowing for fibrillar growth in a reasonable time frame.

3.3.1 Shaking Assay

Development of Shaking Assay. While suppression of nucleation did not occur, shaking gave rise to faster nucleation. Traditionally, recombinant full-length Tau seeds require eight days of stirring to develop fully formed seeds[66]. When using identical concentrations, but subjecting the monomer protein to cycles of shaking and resting, growth can be identified as early as five hours, with complete growth in 48 hours. 3R and 4R Tau grew differently under shaking conditions: hTau23cl aggregated efficiently at 800 RPM shaking, and hTau40cl grew well with shaking speeds of 1200 RPM. When using the Thermomixer R 1000 RPM was seen to efficiently aggregate both hTau23cl and hTau40cl (Figure 10).

When monitoring aggregation in the FLUOstar Omega by ThT, shaking was used at a different rate. This instrument has double orbital shaking with a max speed of 800 RPM. The 700 RPM double orbital setting was used to monitor whether or not polyamines would allow for nucleation and growth of hTau40cl and Aβ42. Shaking was used for faster nucleation of recombinant material. Heparin clearly allowed for nucleation to occur in Tau, while the polyamines had less success (Figure 11). Growth was barely

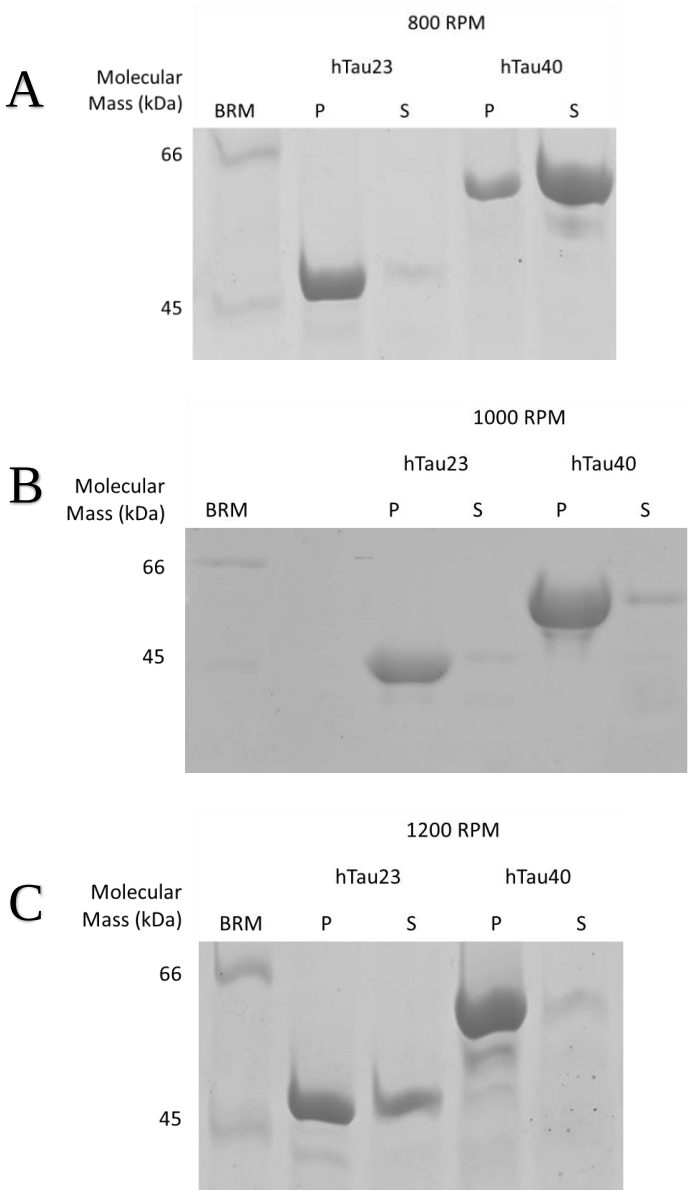

Figure 10: Nucleation Using Different Shaking Speeds. After 48 hours of incubation at 37°C with cycles of 30 seconds shaking and 30 seconds resting show that (A) with a shaking speed of 800 RPM, hTau23cl was fully aggregated, but hTau40cl was not. (B) Both hTau23cl and hTau40cl fully aggregated at 1000 RPM. (C) at 1200 RPM, hTau40cl fully aggregated, but hTau23cl did not. Each experiment was run 3 times with results consistent with the gels shown.

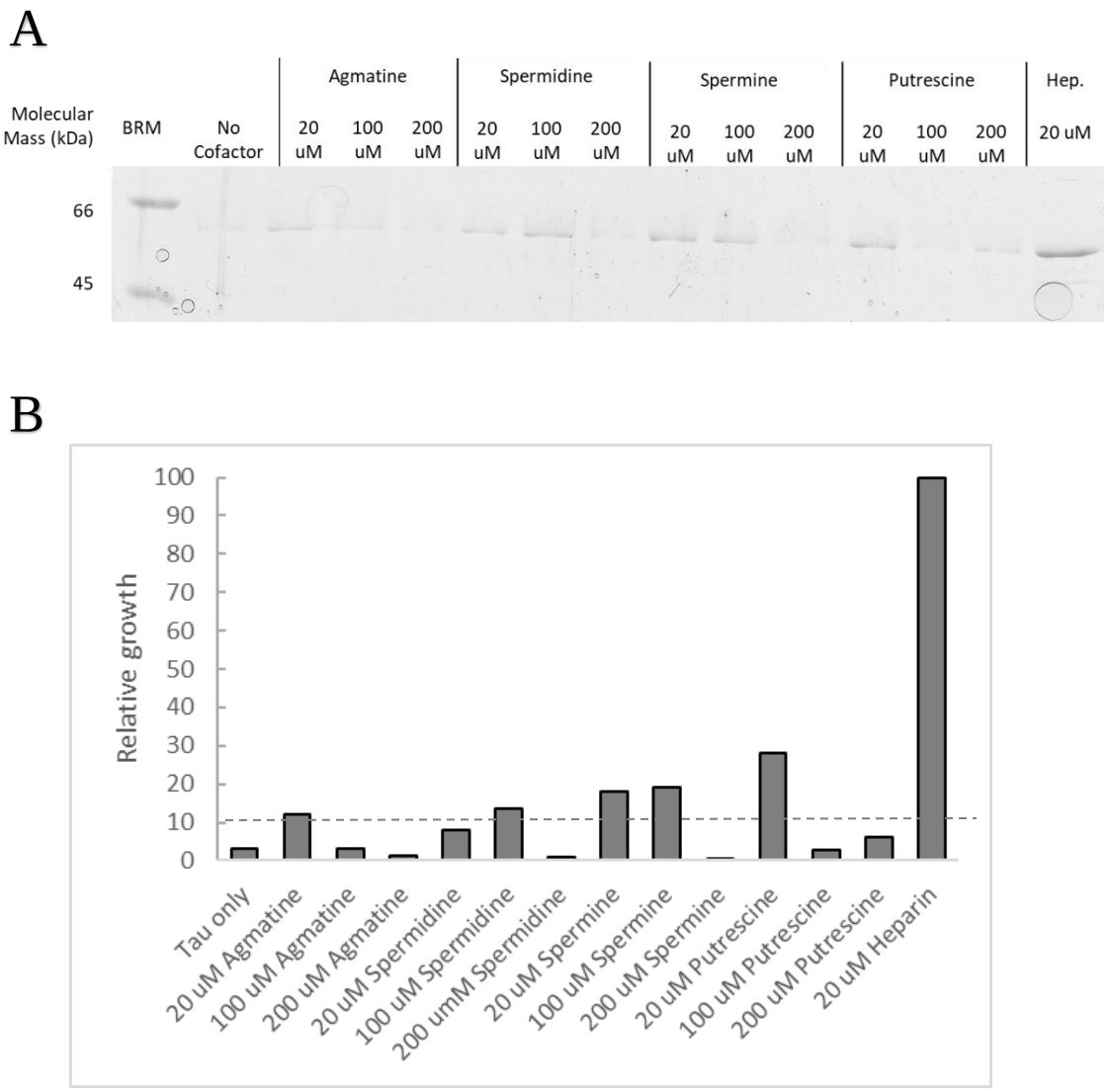

Figure 11 : Nucleation of hTau40cl by Shaking in Presence of Polyamines. (A) The 12% SDS-PAGE run after shaking at 700 RPM double orbital at 37° for 16 hours. In the presence of heparin, hTau40cl nucleated as can be seen on the gel stained with Coomassie blue stain. (B) Densities of the bands were quantified using ImageJ software. Any band above 10% of the growth of hTau40cl and heparin, indicated by the dashed line, is considered nucleation. Since this experiment was only performed once, the reliability of these results has not been assessed.

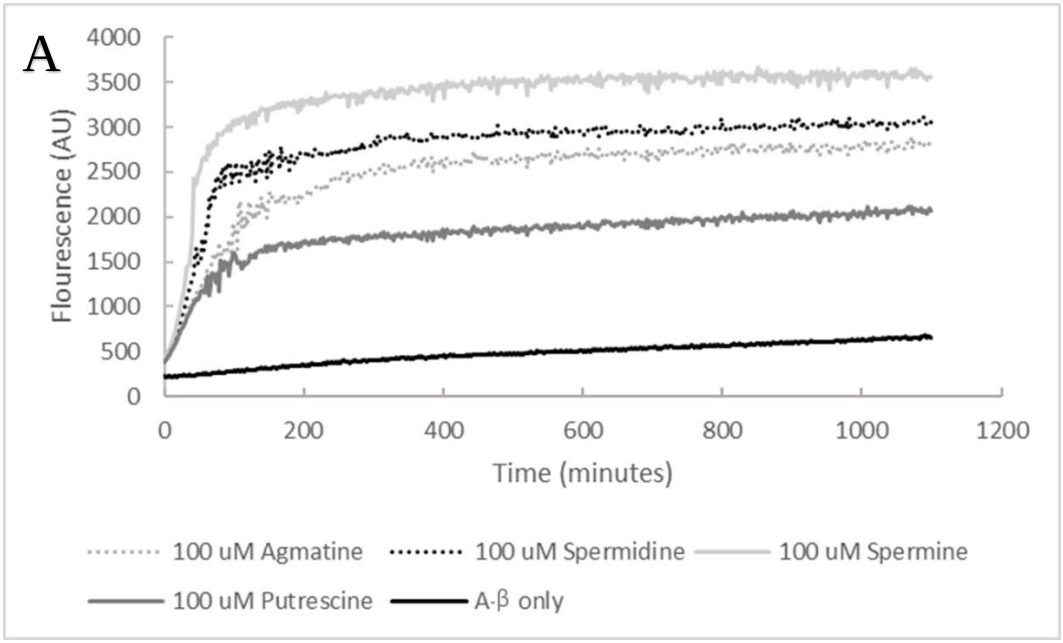

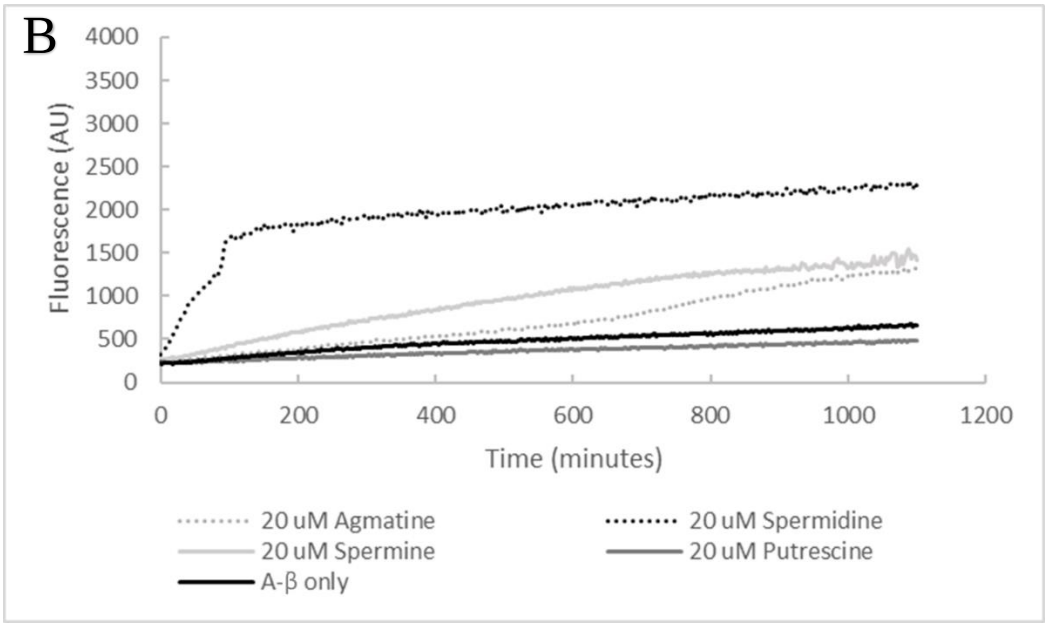

Figure 12: Monitoring Growth by ThT Fluorescence. Using the FLUOstar Omega, fluorescence of ThT was monitored at 30°C and 700 RPM shaking using different concentrations of polyamines as a cofactor for Aβ. (A) was using 100 μM and (B) used 20 μM.

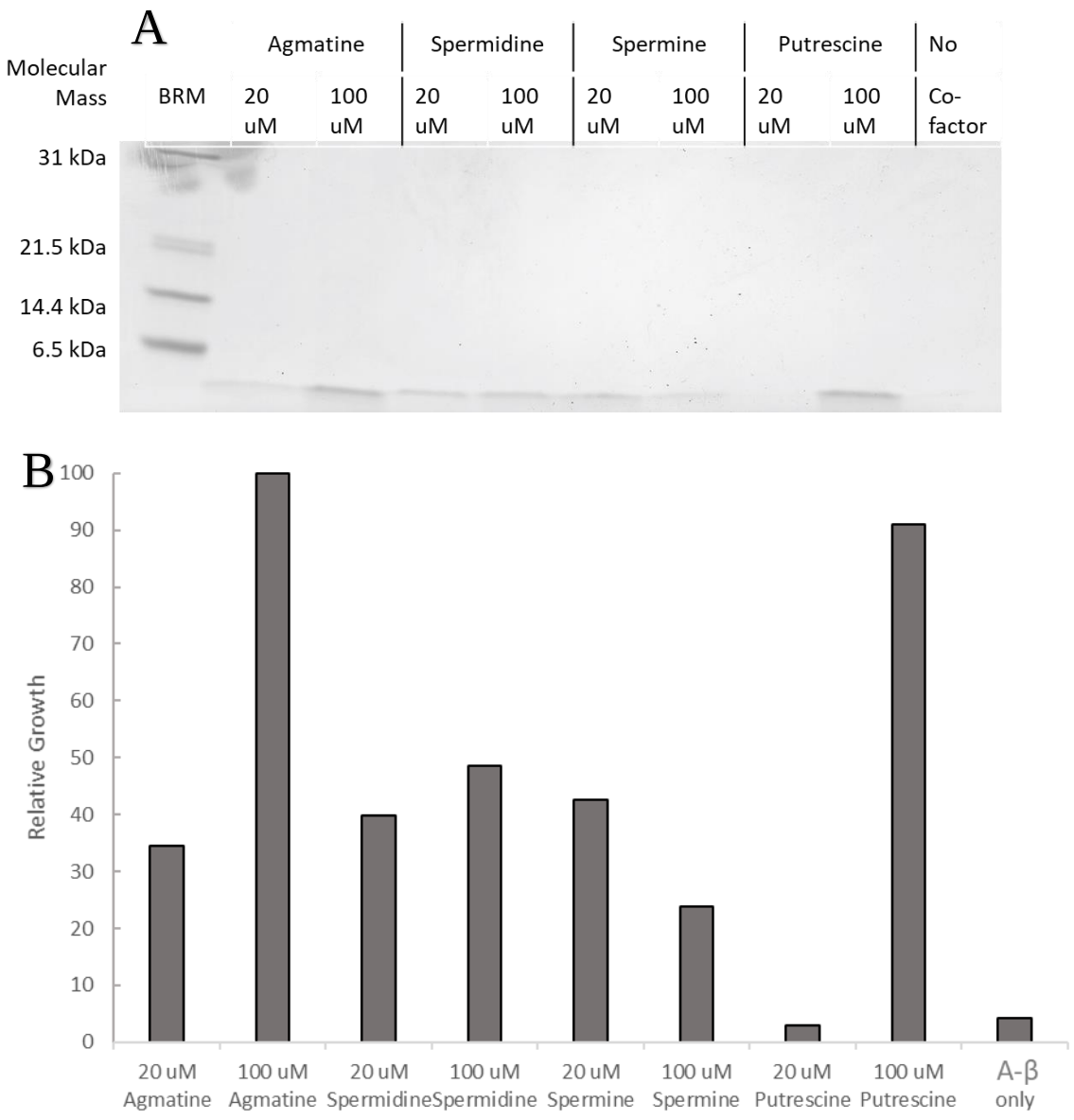

Figure 13: Growth of Aβ42. After the growth was monitored by fluorescence, the reactions were given a high-speed spin and (A) run on a 15% SDS-PAGE gel and stained with Coomassie blue stain. (B) Analysis of the densities of the gel bands were quantified using ImageJ software. Polyamines did increase aggregation of Aβ42, specifically 100 μM of Agmatine and Putrescine.

able to be detected for 100 μM Spermidine, 20 μM and 100 μM Spermine, and 20 μM Putrescine, but strong growth did not occur.

Because Tau requires a cofactor, and Aβ42 is more hydrophobic, the nucleation of Aβ42 is an event that happens more readily than that of Tau[70]. When performing the shaking assay, Aβ42 was incubated at 30°C instead of the typical temperature of 37°C (Figure 12). Since Aβ42 is a much smaller peptide and difficult to see on a 15% gel (Figure 13), ThT fluorescence was monitored on the FLUOstar Omega and a picture of improved aggregation appears with the addition of polyanions.

Limitations to Shaking Assay. When using the shaking assay to amplify Tau fibrils out of AD tissue homogenate, a limitation of the assay appeared. While shaking for five hours in the presence of recombinant hTau40cl seeds showed amplification, shaking with AD tissue homogenate present showed limited amplification and while shaking an unseeded reaction resulted in spontaneous nucleation (Figure 14). A paired t-test showed that there was no significant difference between reactions seeded with tissue extract and unseeded reactions (n=5, p=0.4622). There was a significant difference between monomer and 1% seeded amplification (p=0.0148) and between 1% seeded amplification and AD extract seeded amplification (p=0.0109).

3.3.2 Salt Concentrations

Because of the electrostatic interactions between Tau and the polyanionic cofactor used, altering salt concentrations could influence the way Tau nucleates and grows *in vitro*[71, 59]. Although higher NaCl concentrations suppress nucleation, as the concentration of NaCl increases, growth is diminished (figure 15A). When looking at lower

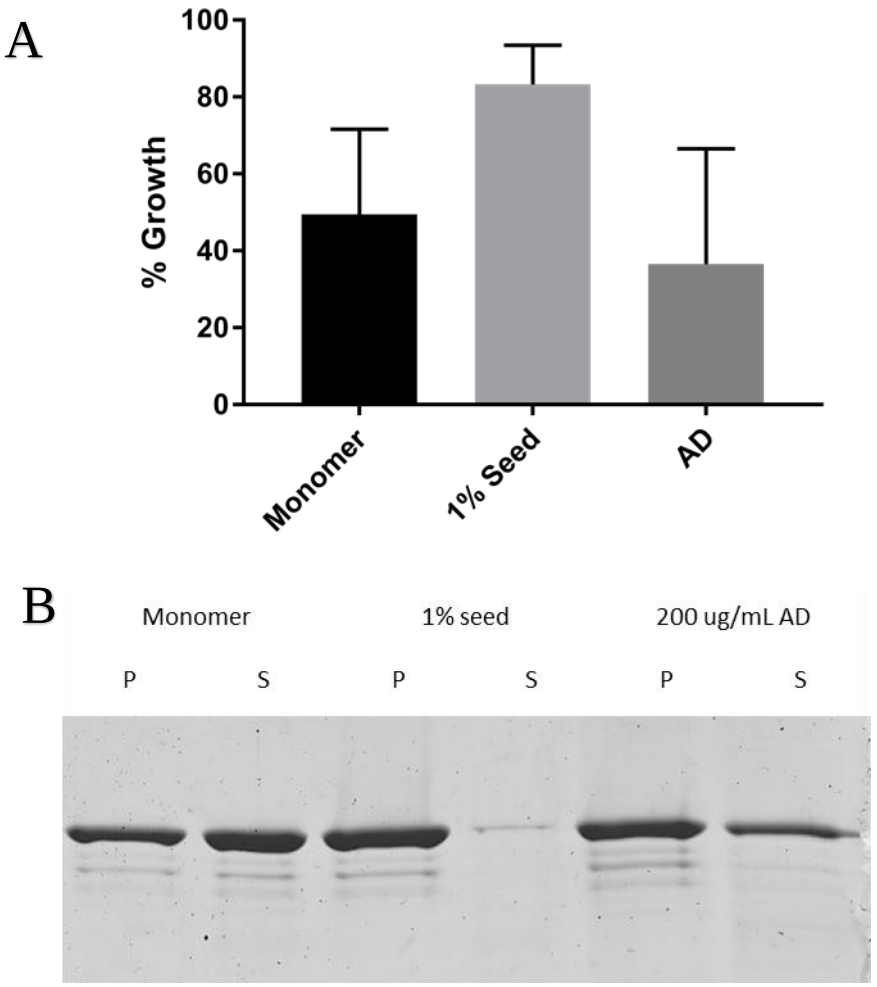

Figure 14: Limitation of Shaking Assay. Using AD brain homogenate showed a limitation of the shaking assay. (A) Quantification of percent growth on SDS-PAGE gels stained with Coomassie blue stain and calculated with ImageJ for monomer only control, 1% seeded reaction, and AD seeded reaction (n=5, error bars represent standard deviation). There is no significant difference between monomer nucleation and AD seeded growth (p=0.4622). (B) A representative SDS-PAGE gel used for quantification.

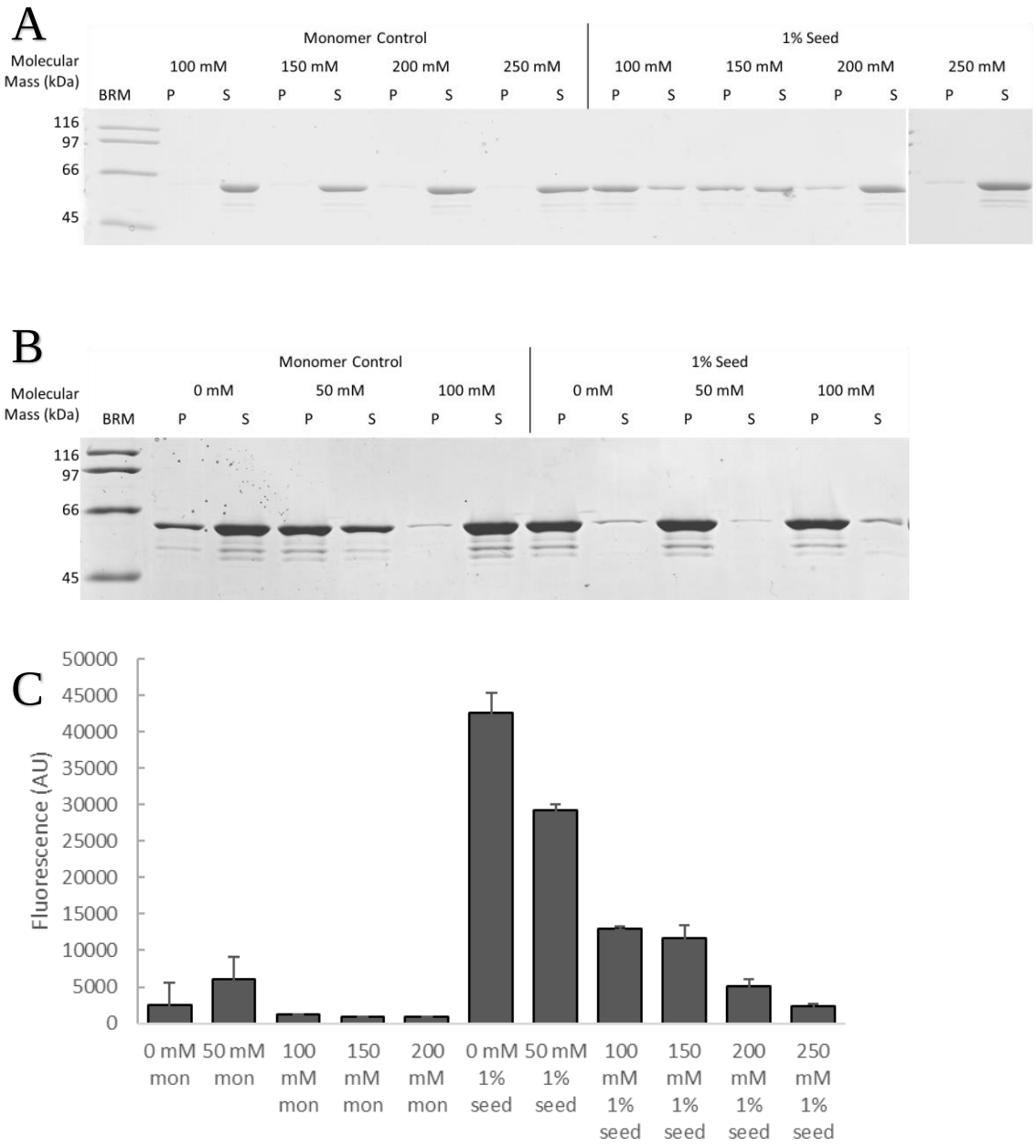

Figure 15: Varying NaCl Concentrations. (A) and (B) show the spin down after 40 cycles of sonication and incubation run on a 12% SDS-PAGE gel and stained with Coomassie blue stain. The graph (C) is the ThT flourescence at the end of 40 cycles Excitation at 440 nm, emission at 480 nm, n=4. Error bars are standard deviation. Two out of four wells of 50 mM NaCl underwent spontaneous nucleation. Only one of four of the 0 mM NaCl experienced spontaneous nucleation.

concentrations of NaCl growth occurs quickly but spontaneous nucleation of the monomer occurs in about 50% of the individual wells for zero and 50 mM NaCl (figure 15B). This data confirms that the standard concentration of 100 mM NaCl is an appropriate concentration for allowing growth while suppressing nucleation of hTau40cl monomer.

3.3.3 Cofactors

Polyanionic cofactors are necessary to allow for aggregation of Tau[33], which has an overall positive charge under physiological conditions[72]. The single strand RNAs Poly(U) and Poly(A), double strand Poly(U/A) RNA, and Poly-glutamate peptides were all compared to heparin during a seed formation experiment. The reactions included 10 μM hTau40cl and one of the five mentioned cofactors. After 24 hours of shaking in cycles of 30 seconds at 1000 RPM followed by 30 seconds of resting, the reactions were centrifuged and compared to one another by assessing the percentage of Tau present in the pellet, or fibrillar Tau. All five cofactors provided similar degrees of aggregation (between 50% and 75%) as seen in figure 16.

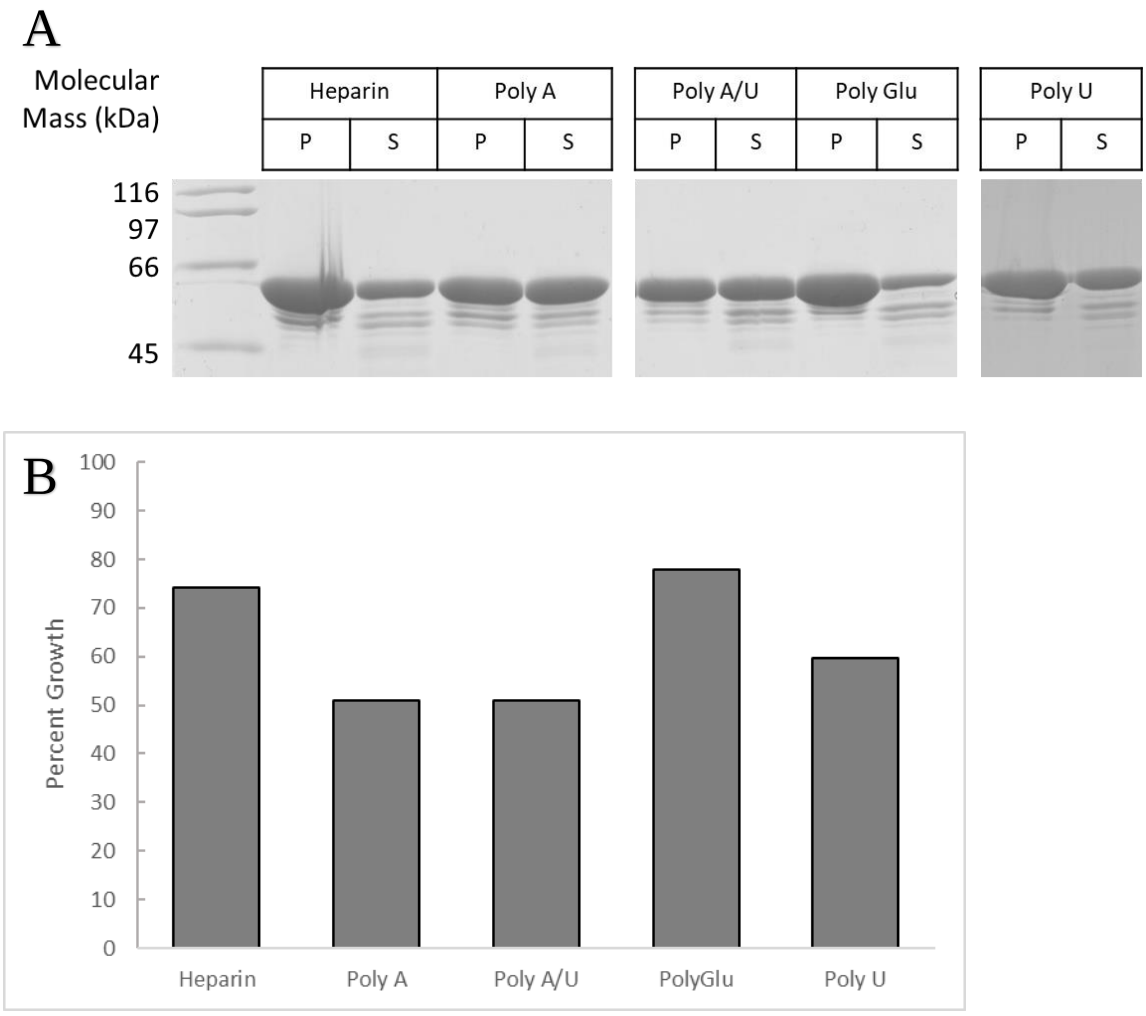

Figure 16: Anionic Cofactors. After 24 hours of shaking, all cofactors induced nucleation and showed similar amounts of growth. (A) shows the 12% SDS-PAGE gel stained with Coomassie blue stain and (B) shows the quantification of the gel bands using ImageJ.

3.4 Applications of Amplification

3.4.1 Differences Among Tauopathies

This assay can be used not only for detection, but also to differentiate between diseases. AD is known to be a tauopathy that aggregates with all six Tau isoforms and PSP aggregates only contain the three 4R Tau isoforms. Undiseased brain tissue as well as AD and PSP tissue were subjected to 30 rounds of sonication and incubation in the presence of hTau23cl or hTau40cl. These reactions were run on an SDS-PAGE gel and the particular isoforms that aggregate are shown in figure 17. The control tissue shows no aggregation for either hTau23cl or hTau40cl. AD shows aggregation in both hTau23cl and hTau40cl. PSP, a 4R tauopathy, shows aggregation of only hTau40cl, and not hTau23cl. Using seeds derived from these aggregation reactions, a seeded assay was monitored for 125 min using ThT. In figure 18, 10% seeds from the amplified AD tissue show reliable growth for both hTau40cl and hTau23cl, while PSP amplified seeds only show growth of hTau40cl in a 125-minute interval. A final difference can be shown in the degradation of fibrils by proteolysis. The aggregates templated by seeds from amplified hTau40cl on AD tissue degrades much more quickly by Proteinase K proteolysis than the hTau40cl aggregates with seeds from PSP extract (Figure 19).

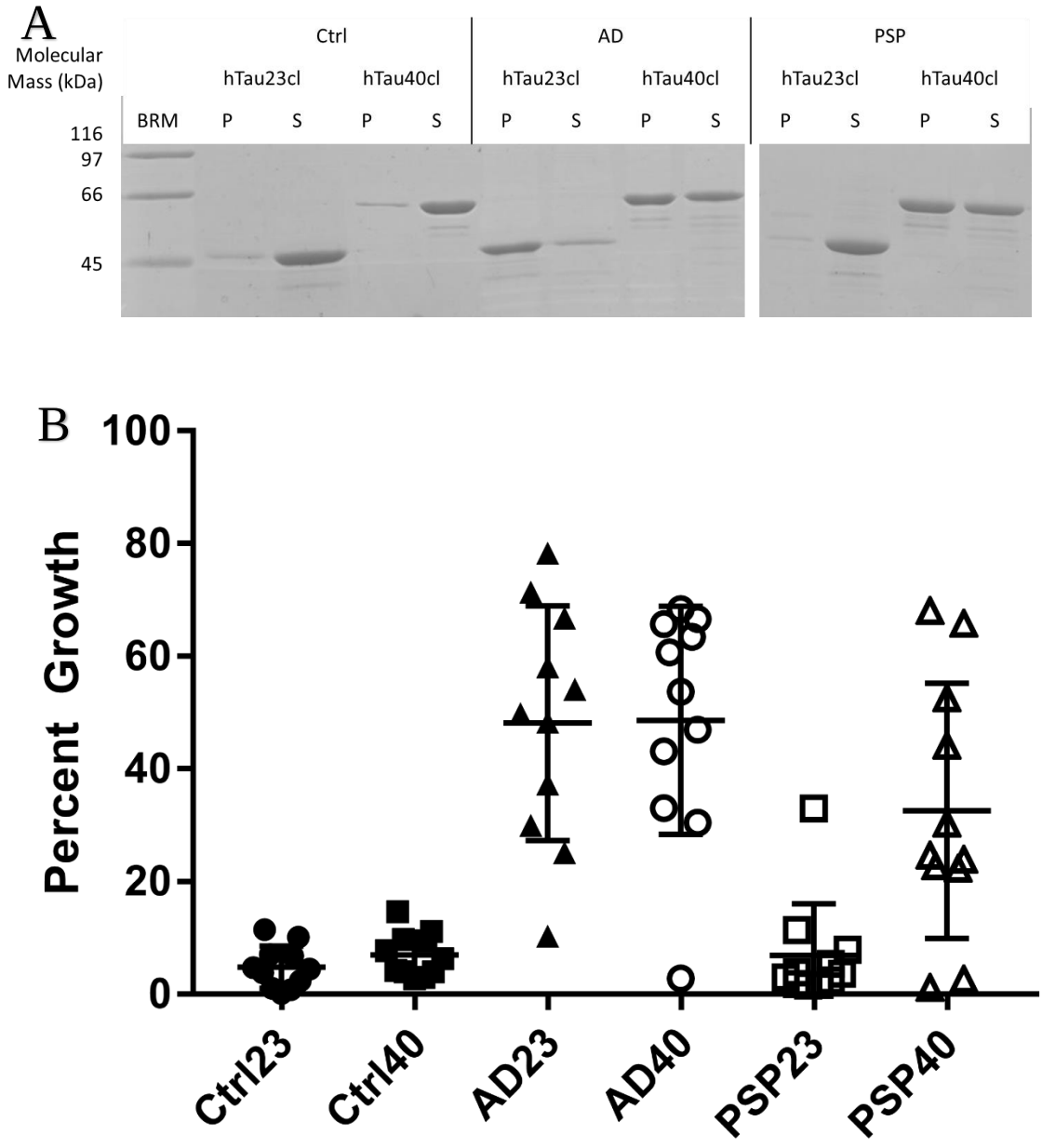

Figure 17: Amplification of AD vs. PSP. (A) After 30 cycles of sonication and incubation, a difference in the growth patterns is shown via a 12% SDS-PAGE gel with Coomassie blue staining. (B) Undiseased control extract shows no growth compared to the growth of AD in the presence of hTau23cl and hTau40cl ($p<0.001$). PSP extract seeded hTau40cl significantly better than hTau23cl ($p=0.004$). There was no significant difference between the growth of hTau23cl on PSP and on undiseased control extract ($n=11$).

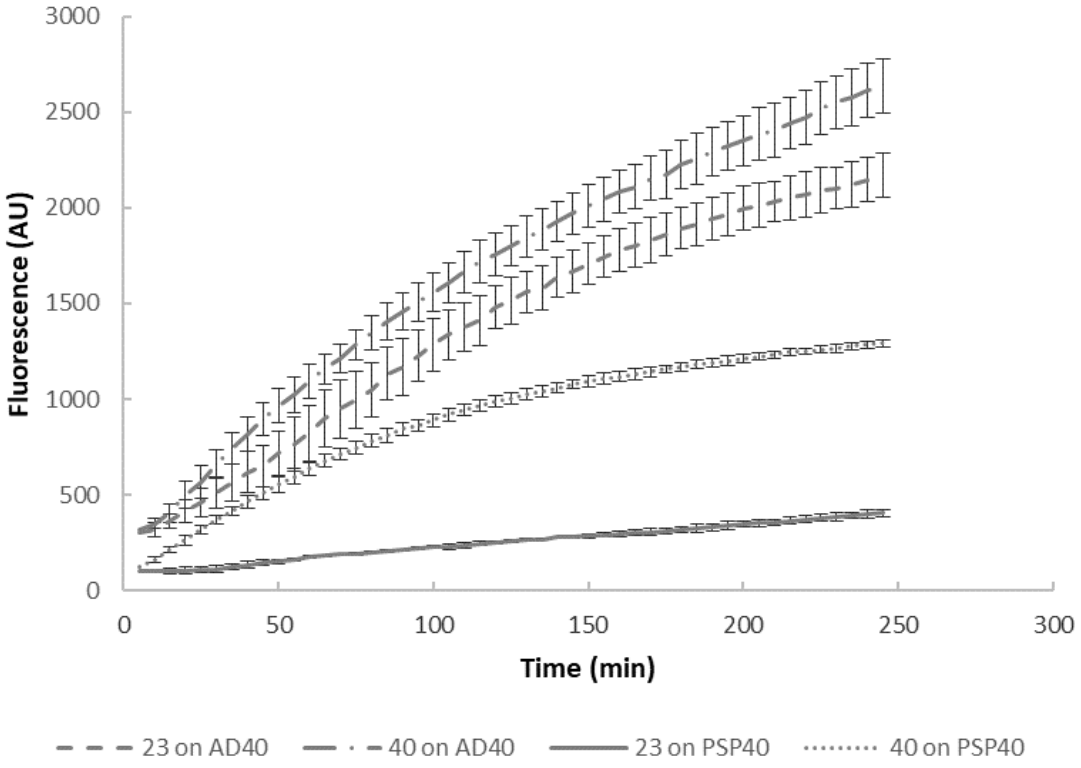

Figure 18: Seeded Reaction of Amplified Fibrils. 10% seeds from hTau40cl amplified on AD and PSP were added to solutions of both hTau23cl and hTau40cl and incubated at 37° for 125 minutes. Excitation occurred at 440 nm and emission at 480 nm. All seeded reactions show growth except hTau23cl on seeds from PSP amplification. Error bars represent standard deviation, n=3.

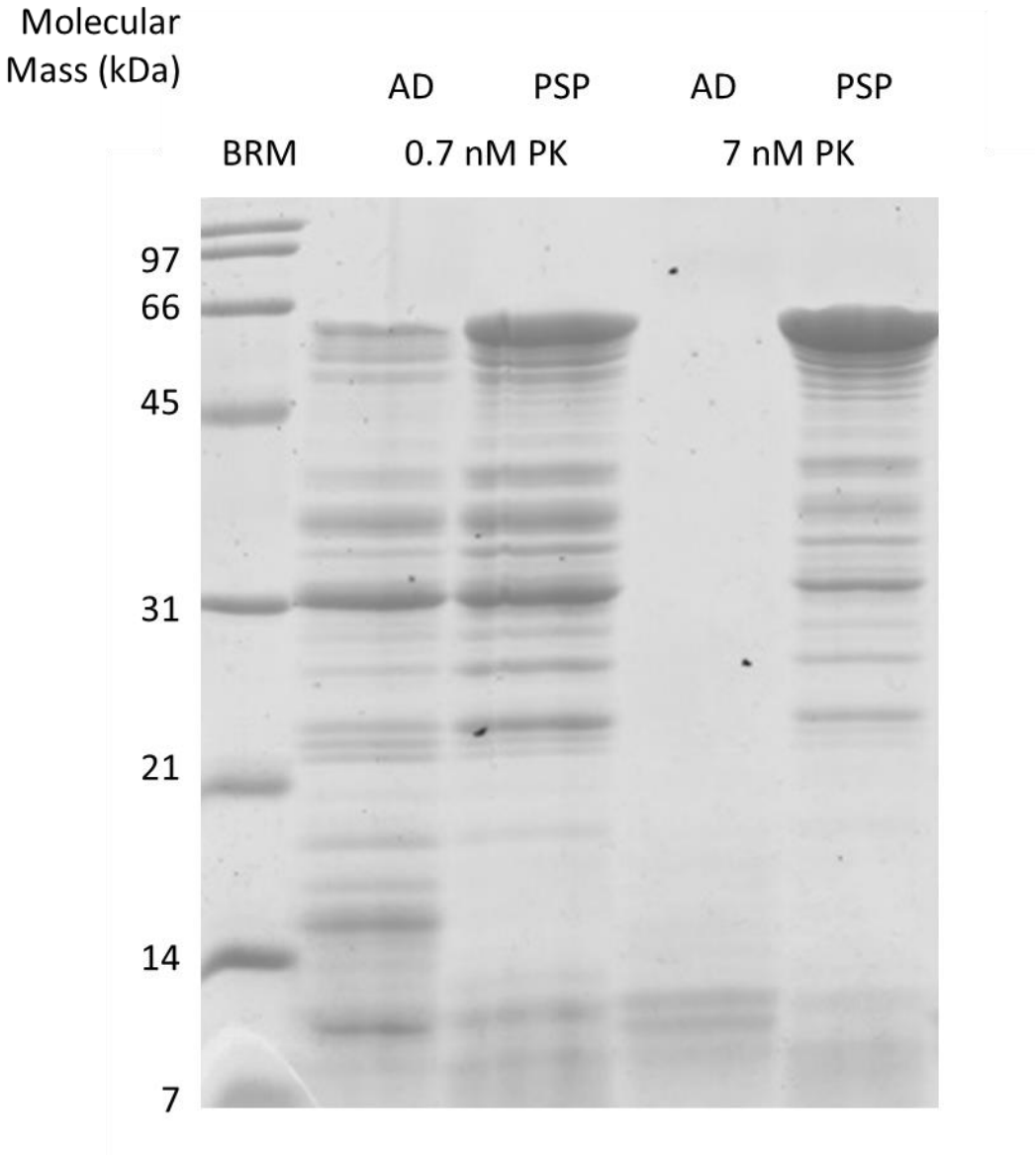

Figure 19: Proteinase K Digestion of AD and PSP Amplified Fibrils. When amplified fibrils from tissue extracts are subjected to proteolysis, the selected conformation of amplified AD fibrils degrades at a faster pace than the selected conformations of amplified PSP fibrils. 10 μM hTau40cl was subjected to PK digestion at the indicated concentrations and run on a 12% SDS-PAGE gel stained with Coomassie blue stain.

3.4.2 Blockage of Aggregation

This assay can also be used to further investigate proteins that have promise in blocking fibril growth of recombinant Tau. MAP2 has been shown to block the growth of recombinant fibrils formed *in vitro*. In work unpublished as of this date, Michael Holden with the Laboratory of Martin Margittai has shown that trMAP2c and trMAP2d can block growth of K18 when incubated quiescently with recombinant K18 seeds. To determine the effect trMAP2c and trMAP2d have on seeding of authentic fibrils, they were subjected to 30 cycles of amplification in the presence of homogenized AD tissue. Two different AD samples (AD21 and AD110) were used, both from the cerebral cortex. The source from which each brain sample originated was pathologically diagnosed with AD. When subject to amplification cycles in the presence of trMAP2c and trMAP2d decreased capability for aggregation is shown (Figure 20). For AD21 amplified in the presence of trMAP2c, aggregation was only 22% (±6) of the growth of hTau40cl on AD21 and in the presence of trMAP2d aggregation was 17% (±5) of said growth. For AD110 amplified in the presence of trMAP2c, aggregation was 53% (±8) of the growth of hTau40cl on AD110 and in the presence of trMAP2d aggregation was 206% (±7) of said growth. In each of the cases, the difference is statistically significant ($p<0.0001$). In comparison, undiseased extract shows no amplification when subjected to the same number of cycles.

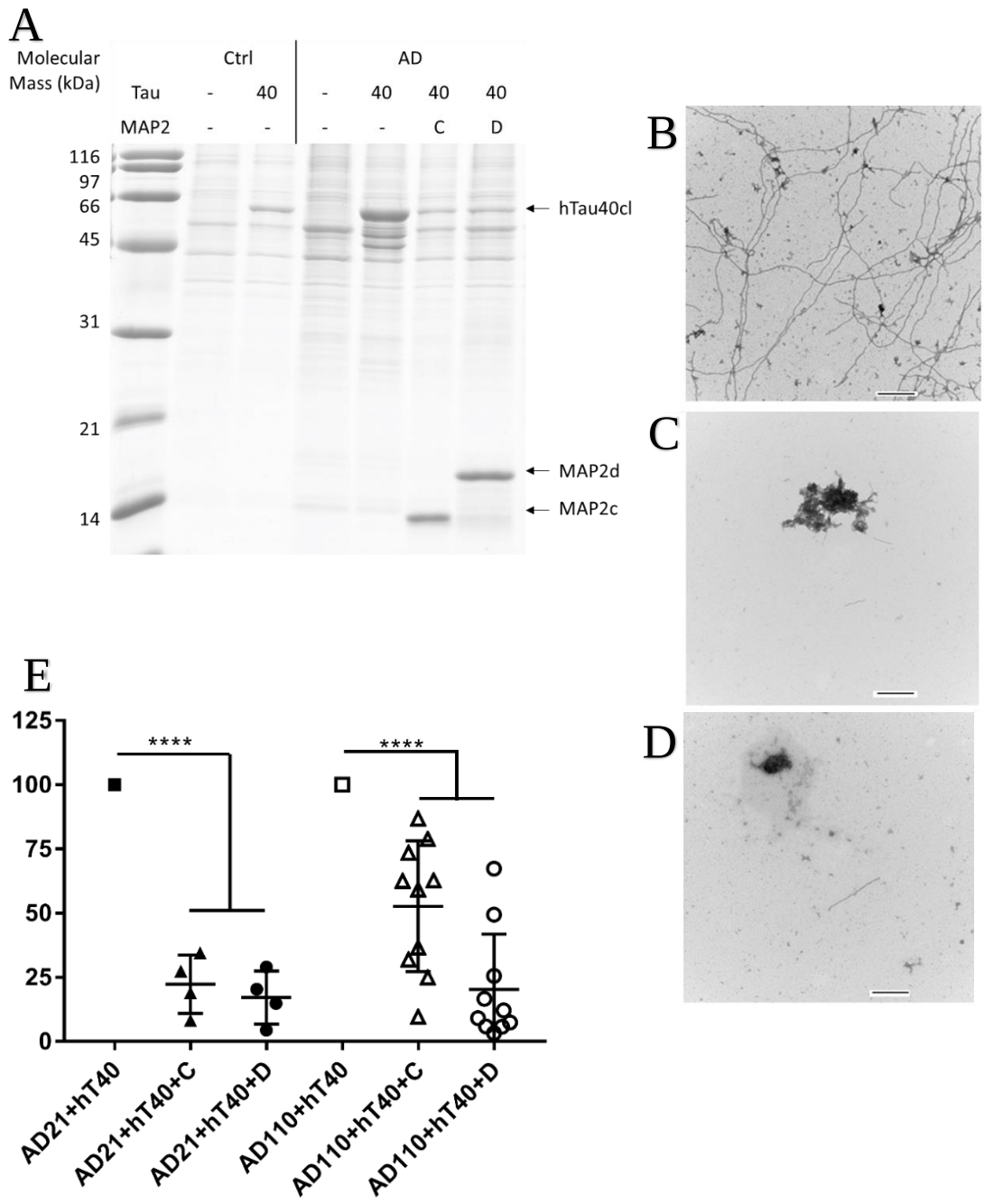

Figure 20: Blockage of Tau Aggregation by MAP2. (A) A representative 15% SDS-PAGE gel stained with Coomassie blue showing the blockage of AD21 by MAP2c and MAP2d. EM images of negatively stained Tau samples showing growth in the absence of MAP2 (B), in the presence of MAP2c (C), and in the presence of MAP2d (D) Scale bars = 500nm. (E) the accumulation of data showing significant blockage of Tau growth using MAP2c and MAP2d with two different AD extract samples ($p<0.0001$).

Chapter Four: Discussion

4.1 Amplification Using Sonication

Seeded reactions with fibrils sonicated only once at the beginning of the process and incubated can show growth, with enough seeds present (Figure 7). Using hTau40cl, seeds must be at 100 nM to be able to see that a seeding event has taken place. Seed concentrations of 100 nM identify some growth in hTau23cl, while higher concentrations show better results. When additional sonications are added to the process, growth occurs much more rapidly and seeds as low as 10 pM can be amplified in both hTau23cl and hTau40cl (Figure 7). This significant increase in seeding is likely due to the increased number of seed ends available to the monomer on which to grow. If the seeds are uniformly sonicated initially, a static number of ends will be available for the monomer to add on to, with fibrils growing longer and longer. Adding periodic sonications to the incubations allow the fibrils to grow in the 30-minute incubation period and fractures the fibrils offering an increase in available ends for monomer to add on to. Each successive sonication adds even more ends on which monomer can grow, allowing for amplification of as few as 400,000 fibril seeds.

The rational for this follows. The amount of seed added is 0.0001% of 10 μM in 200 μL wells, which will be in the range of 10^{-15} moles, or around a fmol or 10^{8} monomer units. When seeds are sonicated for two minutes at the beginning of an experiment, they

are broken down into fibrils about 60 nm long on average, with a positively skewed distribution containing fibril seeds of up to 400 nm[73]. The above experiments began with a 30-second sonication. If the estimate is that each monomer in a fibril is 0.5 nm apart and there are two monomers per layer[74], there would be approximately 250 monomers per fibril. Thus 10^8 monomer units divided by 250 monomers per fibril gives 400,000 fibril seeds. Due to the shorter seed sonication, this number could be considerably lower.

Aggregation of hTau23cl requires a larger number of seeds because hTau23cl does not aggregate as readily as hTau40cl[75]. The minimum detectable amount of seeds for hTau23cl in quiescent incubation for 15 hours is 100 nM. When cycles of sonication and incubation are added, the detection limit of hTau23cl is considerably improved with 10 pM seeds showing growth, and full growth seen with as few as 100 pM seeds.

The difference in the aggregation behavior of hTau23cl and hTau40cl is not surprising because the 3R and 4R Tau isoforms have long been shown to have different aggregation patterns both in disease and *in vitro*[76,16]. The truncated isoforms of Tau have long been shown to have an asymetric seeding barrier with K18 being competent to grow on seeds of K19, but K19 not able to grow on K18. Tauopathies are considered either 3R, 4R, or mixed fibril diseases. PSP preferentially grows 4R Tau and 3R Tau is aggregated in PiD also indicating that some differences in aggregation are expected.

Using a biological sample for amplification offered a new set of possible complications. The homogenized tissue contains more components than the highly purified recombinantly seeded reactions. These additional components include a variety of additional proteins, RNA, DNA, metal ions, small molecules, and lipids. The

membranes were disrupted using the detergent Triton X-100 and sonication during the homogenization step allowing the contents of the individual cells to become part of the solution. All tissue used in the assay are from the cortex and showed indistinguishable banding patterns on an SDS-PAGE gel, but the tissues were pathologically different. Undiseased brain tissue was pathologically determined at autopsy to have no Tau fibrils and be confirmed Braak stage 0 and AD tissue used was pathologically determined at autopsy to have tangles of Braak stage V or VI.

Amplification of hTau40cl and hTau23cl over 30 cycles show amplification in tissue from AD tissue and minimal to no amplification from undiseased tissue. The 200 μg/mL of total protein concentration from the tissue that is included in the solution contains enough seeds to be reliably amplified after the cycles were complete. When the amplified fibrils are looked at with EM, the fibrils that have grown typically appear to be attached to debris from the brain tissue homogenate (Figure 9B and C). *In vivo* these fibrils could be attached to specific cellular components, or the homogenization process could have caused this effect. EM images of fixed AD tissue show fibrils contained in neuropil threads to be surrounded by debris[77].

Occasionally undiseased tissue would show growth after the completion of the cycles (Figure 21). The assay, being sensitive enough to detect a small number of recombinant seeds might suggest that though the undiseased tissue was pathologically determined not to contain fibrils, some tissues did in fact have small amounts of aggregates. This false positive could also be attributed to contamination or spontaneous nucleation. AD tissue that is taken from the cortex can be reliably amplified, however

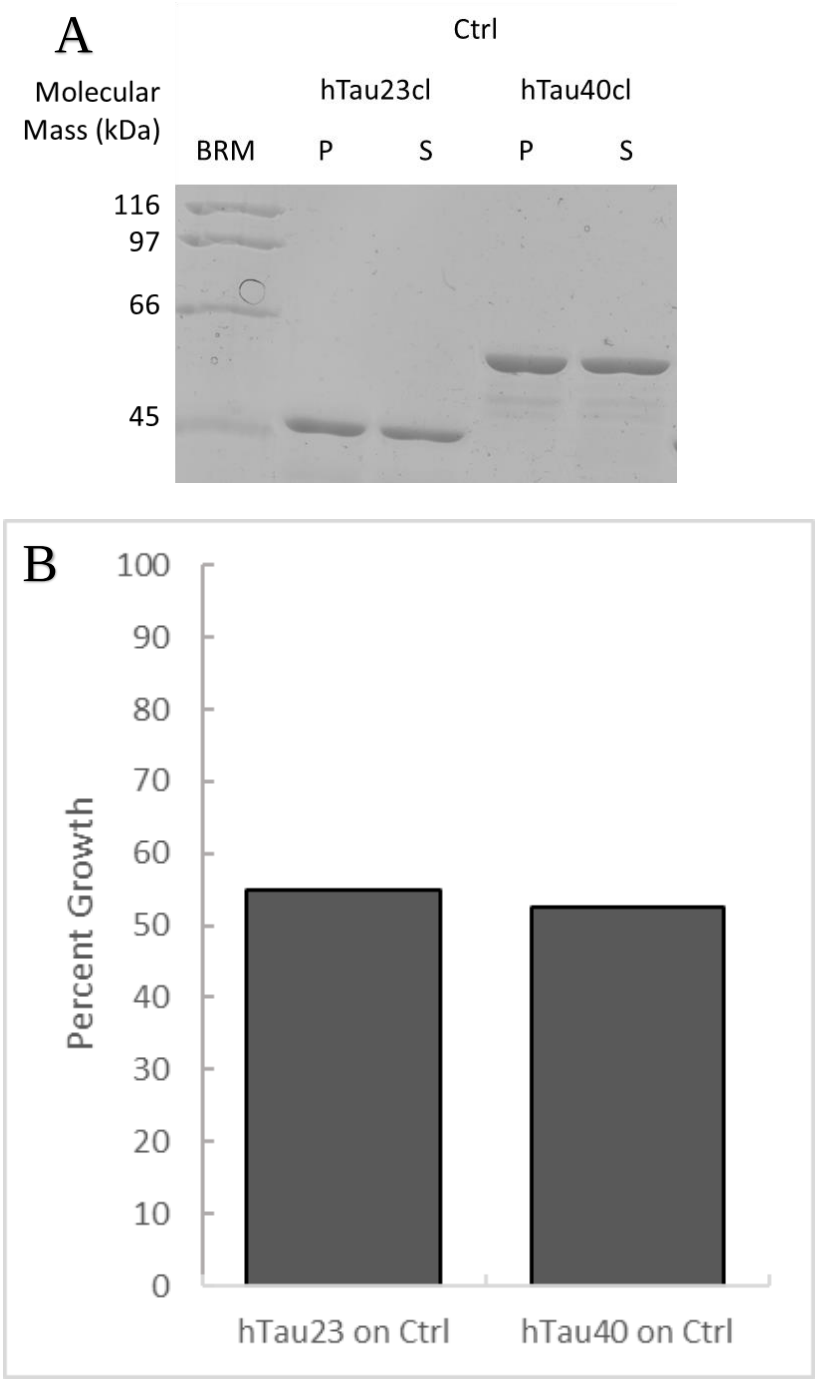

Figure 21: Occasional Growth with Control Tissue Extract. (A) Representative SDS-PAGE gel stained with Coomassie blue showing growth in undiseased control tissue extract. (B) Percent growth of Ctrl extract was calculated from densities on SDS-PAGE gel shown.

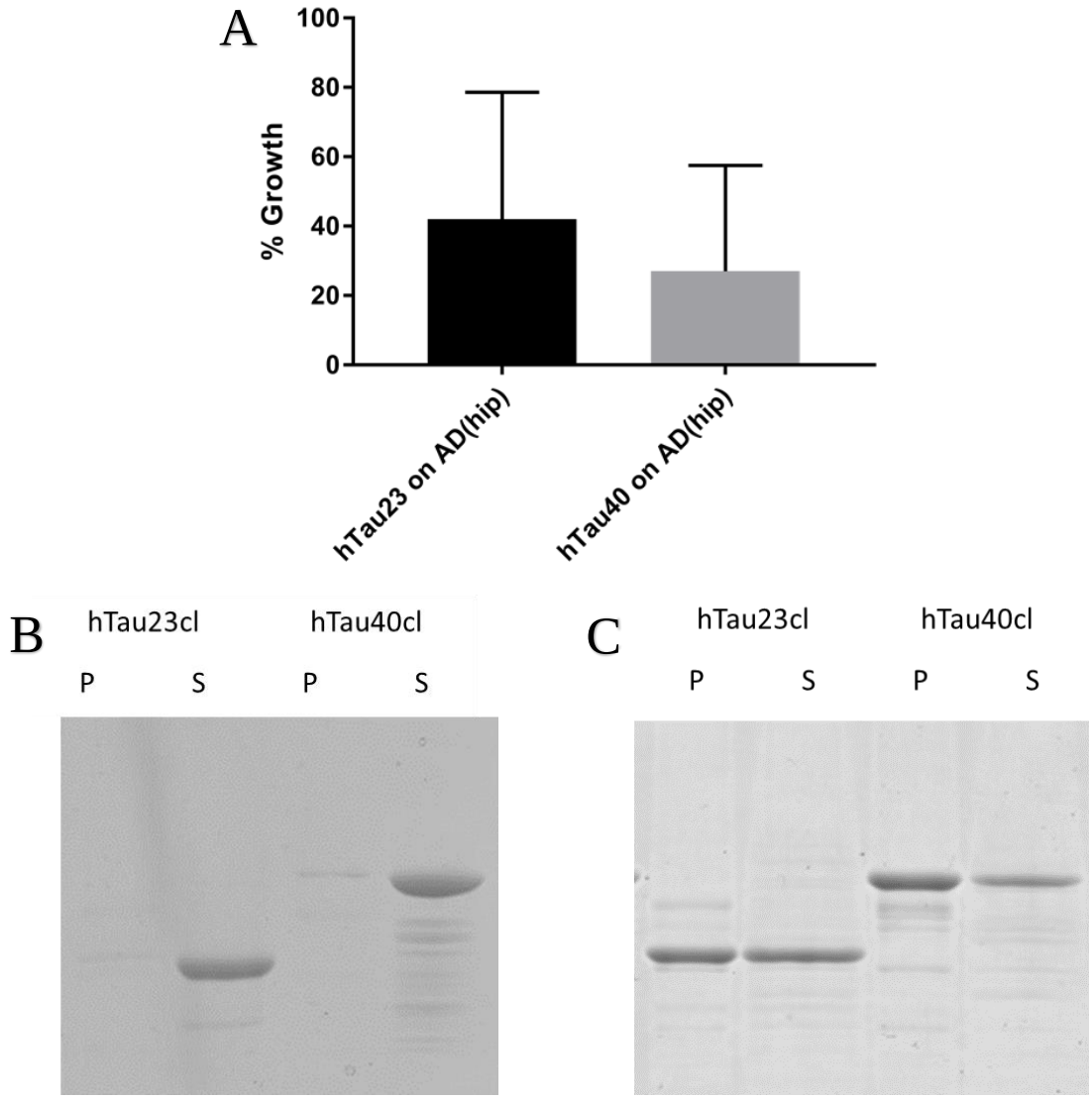

Figure 22: Amplification from Hippocampus Extract is Inconsistent. (A) Percent growth of AD extract from hippocampus extract from a single biological source was calculated from densities on SDS-PAGE gels with Coomassie blue stain using ImageJ (n=5, error bars are standard deviation). Representative gel showing no growth (B) and moderate growth (C).

tissue from the hippocampus shows some evidence of amplification, but not consistently (Figure 22).

4.2 Areas of Improvement

4.2.1 Shaking

In developing the shaking assay, the shaking conditions used were different for each instrument. For the Thermomixer R, a shaking speed of 1000 RPM was settled upon for optimal growth and on the FluoStar Omega, 700 RPM double orbital was the most efficient setting used. Shaking was not ideal for biological samples (figure 14). Growth of recombinant protein in the presence of recombinant seeds was robust and showed full growth in 4 hours of shaking cycles. Spontaneous nucleation of unseeded material occurs before the detection of amplification in the AD seeded reactions. The extra components present in the AD tissue homogenate could prevent shaking from amplifying the fibrils, or sonication, being a more aggressive disruption could break apart the brain derived fibrils more efficiently than shaking.

The shaking worked very well for monitoring for nucleation of recombinant protein. Nucleation of hTau40cl in the presence of heparin was successful and occurs at a much faster pace than the traditional stirring method for making seeds. Shaking is a more aggressive mixing than stirring and likely allows for more opportunities for the necessary meeting of protein and cofactor required for nucleation to occur and shortening the lag phase. Tau fibrils created in this way are likely fractured more often, offering more ends for the monomer to grow onto.

Positively charged polyamines were less successful than heparin as cofactors in the nucleation of hTau40cl however, some effect was seen (Figure 11). Polyamines with Aβ42 however, do increase the rate of nucleation with spermidine and spermine being the most efficient cofactors (Figure 11, 12). This is interesting because it has been shown that natural polyamine levels change in AD[78]. These two polyamines are the longest of those tested and they contained three and four amines respectively separated by either three or four carbon atoms on a flexible backbone.

4.2.2 Salt Concentrations

Varying the salt concentration strongly affected nucleation. At higher concentrations, nucleation was prohibited, which was promising however, growth was also restricted. At lower concentrations, spontaneous nucleation was increased and growth was abundant. When looking for spontaneous nucleation, both the salt free reactions and the 50 mM NaCl reactions showed some growth. The higher aggregation in the 50 mM reaction can be explained due to the fact that nucleation is a spontaneous event (Figure 15). At lower NaCl concentrations, nucleation can occur more easily[71]. There are fewer anions and cations in solution which could interfere with the attraction of positively charged Tau and negatively charged heparin. In this experiment, the nucleation of the 50 mM NaCl reaction occurred slightly faster than that of the no NaCl reaction. The important thing to note at lower NaCl concentrations is that spontaneous nucleation is more likely to occur, and are not ideal for amplification of small amounts of seeds.

As NaCl concentration increases, the ability for growth decreases. Nucleation is more difficult at high concentrations likely due to the increase in charge distribution of

the solution. More ions in solution can prevent the positive charge of Tau and the negative charges on heparin from lining up in a manner which creates the nucleus. At very high salt concentrations, one would predict that each of the positive or negative charges along the protein and cofactor would be neutralized with a corresponding anion or cation in solution. This allows for a greater number of cycles to occur, however, seeded reactions at concentrations of NaCl higher than 200 mM also show no growth. NaCl concentrations between 100 mM and 150 mM appear to be ideal for this assay.

4.3 Application of Assay

4.3.1 Differences in Disease Fibrils

The amplification assay can be used in a variety of ways. Showing differences between different brain tissues is the first. When subjected to repeated cycles of sonication and incubation pathologically different tissue extracts show different patterns of amplification. As shown above, undiseased, tangle free tissue homogenate does not amplify hTau23cl or hTau40cl. Since Tau fibrils are not seen in undiseased tissue, this is the expected outcome. AD extract is shown above to amplify both isoforms of Tau. Tau fibrils in AD contain both 3R and 4R tau, so this result is also expected. Amplification of PSP also lined up with the hypothesis and hTau40cl was amplified while the amplification of hTau23cl was minimal. In the late 1990s, Buée et al suggested that specific mutations in the MAPT gene caused Exon 10 to produce a higher level of 4R Tau[79]. This idea led to the belief that 4R Tau was recruited into aggregates in PSP because there was more 4R Tau available. In the first decade of the 2000s, it was shown that 3R tau and 4R tau are present in similar concentrations in the brains of those with

PSP[80,81]. Most recently, cell lines expressing 3R Tau did not show aggregates when exposed to fibrils isolated from PSP tissue, but cell lines expressing 4R Tau showed robust growth[82]. This points to a mechanism where the conformation of PSP fibrils are able to recruit only 4R and not 3R Tau. The data presented in the present work agrees with prior work that a conformational preference for 4R Tau in PSP fibrils exists. This preference, which is present in PSP and absent in AD point to differences in aggregation behavior between the two diseases.

It is possible that amplification shows a preference for specific fibril conformations in diseased brain tissue. This preference does not negate the fact that conformational differences exist in tissue. Repeated sonications and incubations likely select for the most fragile or faster growing conformations[73]. If two diseases have a similar population of fibrils, one would expect the amplified conformations to also be similar. In the case of AD and PSP, the amplified conformations appear to be quite different. To investigate this difference further, the amplified fibrils of hTau40cl on AD and hTau40cl on PSP were used as seeds for a second reaction. This reaction was monitored via ThT fluorescence. Again, the seeding barrier occurred showing that hTau23cl was prevented from growing on seeds derived from PSP brain while allowing hTau40cl to grow. Growth of both hTau23cl and hTau40cl occurred on seeds amplified from AD tissue.

Amplified fibrils of hTau40cl from each disease source were also subjected to proteolysis. Proteinase K is a protease which selectively cleaves proteins at aliphatic and aromatic AA residues. When similar fibril concentrations were subjected to proteolysis,

the PSP derived fibrils were more quickly degraded than those from AD (Figure 19). This suggests that the fibrils amplified out of AD tissue have more protease resistance than those amplified from PSP tissue. This is likely due to a structural difference between the amplified conformations, however additional experiments are needed to verify the reproducibility of these results.

4.3.2 Blockage of Growth

Blockage can be seen consistently when samples of AD extract and recombinant hTau40cl are subjected to cycles of incubation and sonication in the presence of trMAP2c and trMAP2d. Each of the diseased tissues amplified reliably when no MAP2 was present, and the undiseased tissue failed to amplify. When amplified in the presence of trMAP2c and trMAP2d, less aggregation occurs (Figure 20). More blockage occurs in the presence of trMAP2c and trMAP2d with AD21 extract than the analogous experiments with AD110. There are several possible explanations for this difference. It is possible that the number of aggregates in the AD110 tissue was greater those found in the AD21 tissue. More ends would be offered to the monomer for amplification and amplification could begin before MAP2 has a chance to block fibrillar growth. Structural differences in the amplified conformations could also account for differences. If the selected conformation amplified from AD110 was more fragile or faster growing, more amplification could be occurring before MAP2 can act. Regardless of the reason for differences between tissue samples, there is a significant difference in the aggregation of Tau in the presence and absence of each of the MAP2 isoforms. Of note, trMAP2d at a 1:2 ratio to hTau40cl blocks better than an equimolar amount of trMAP2c:hTau40cl.

Chapter Five: Summary

5.1 Assay Development and Application

In the above work, an assay to detect tau fibrils from small amounts of diseased tissue was developed. The assay can be reliably reproduced using recombinant fibrils to detect fibrils at concentrations as small as 10 pM. This assay can detect fibrils from 20 μg of homogenized cerebral cortex brain tissue. Beyond detection, this assay can show differences in available fibril populations and the efficiency of blocking agents.

5.2 Improving Detection and Differentiation

While developing the assay, several environmental variables were investigated to find conditions that would allow for elongation while suppressing spontaneous nucleation. By using the same solution and subjecting it to shaking instead of sonication, the experimental time to convert PrP to PrP^{SC} was decreased[67]. When the same concept was applied to Tau, spontaneous nucleation occurred more quickly and fibrils were not amplified from brain tissue. The shaking assay can be used to monitor nucleation and form seeds more quickly than the traditional stirred method.

Salt concentration affected both nucleation and growth. Concentrations below 100 mM NaCl allowed for rapid growth, but did not suppress spontaneous nucleation. Concentrations above 200 mM NaCl successfully blocked nucleation, but also prevented efficient growth. The ideal concentration of NaCl for amplification is between 100 mM

and 150 mM. Cofactors were also investigated. Each of the proposed anionic cofactors worked nearly identical to heparin. Since the standard conditions in the Margittai laboratory are 100 mM NaCl and heparin as a cofactor, no changes were made. Other environmental possibilities that could be tested include incubation temperature, pH, and sonication strength and duration. Paul Dinkel and Virginia Meyer did much of the optimization of sonication strength and duration in a previously published work[66]. Going forward, these conditions could be modified and combined to find an even more sensitive method.

Using this assay to look at differences between other diseased tissue samples is another possible direction. Accumulating a variety of samples from multiple diseased and undiseased tissues could begin to shed light on the similarities and differences among tauopathies. It has been shown in this work that AD and PSP recruit hTau23cl and hTau40cl differently in amplification and that AD21 and AD110 have different blockage patterns when amplified in the presence of MAP2. In the future, additional diseases such as PiD, CTE and CBD can be subjected to amplification to determine if the 3R tauopathies, 4R tauopathies, and mixed fibril tauopathies recruit only the isoforms in their classification. Subjecting different areas of the same diseased brain to amplification and comparing the results to one another can also give information about spreading in disease. Finally, comparing the amplification products of different brain tissue with the same pathological diagnosis to one another could offer information about similarities and differences within a single disease.

5.3 Applying Assay to More Accessible Biological Samples

The assay developed here shows promise for detecting even the smallest amounts of fibrils in solution. Exosomes are small vesicles secreted by cells, including neurons, which contain various proteins and RNA[83]. Exosomes are used in signaling and removing unwanted proteins from the cell, frequently ending up in the blood stream[84]. Using antibodies, the Granholm lab has shown that phosphorylated Tau is present in higher concentrations in the blood derived exosomes of those with DS than exosomes from undiseased patients[85]. The Tau identified was identified using antibodies and it was not specified whether the Tau was fibrillar or not. Upon acquiring exosomes from the Granholm lab, they were subjected to amplification, and preliminarily DS exosomes show amplification after 30 cycles (Figure 21). Like the brain tissue, the background of the exosomes was indistinguishable between undiseased and DS exosomes. This is promising because exosomes can be purified from more accessible biological samples.

As this assay becomes more sensitive, several positive and negative outcomes could be possible. With detection at single fibril levels, it may be possible to use a simple blood draw to detect tauopathies. Since Tau begins aggregating in AD decades before the first symptoms are seen, an early detection method might allow for treatment at earlier stages than ever before.

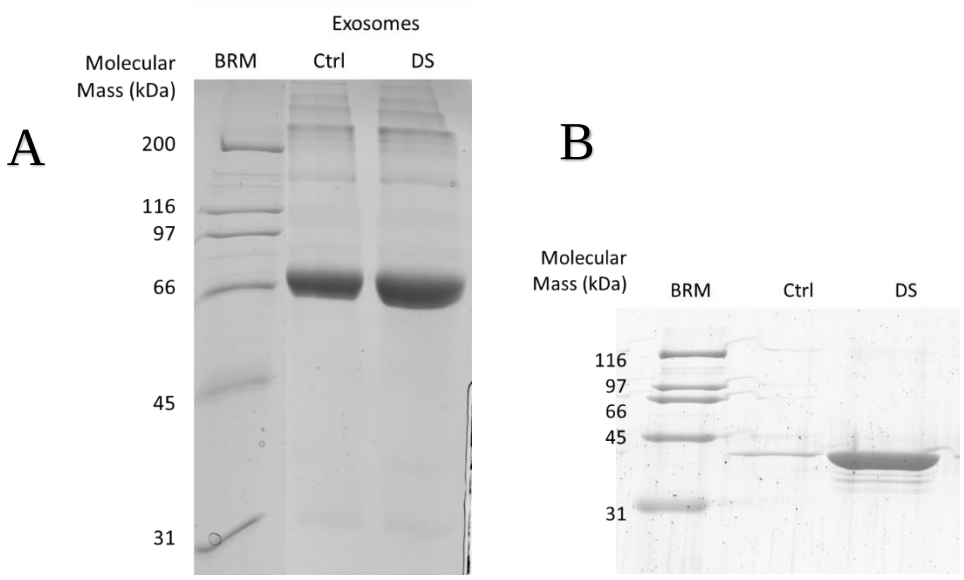

Figure 23: Amplification of Fibrils from Exosomes. (A) The background of undiseased control exosomes is indistinguishable from those of a DS patient. The dark band shown in the exosomes is not Tau. Since the exosomes were purified using a pull-down assay, the most prominent band is likely the pulldown target[85]. (B) The exosomes from DS have shown promising capability of amplification compared to undiseased control exosomes.

References

(1) Mann, D. The Neuropathology of Alzheimer's Disease: A Review with Pathogenetic, Aetiological and Therapeutic Considerations. *Mech. Ageing Dev.* **1985**, *31* (3), 213–255.

(2) Shankar, G.; Walsh, D. Alzheimer's Disease: Synaptic Dysfunction and Aβ. *Mol. Neurodegener.* **2009**, *4* (1), 1–13.

(3) Braak, H.; Braak, E. Neuropathological Stageing of Alzheimer-Related Changes. *Acta Neuropathol.* **1991**, *82* (4), 239–259.

(4) Villain, N.; Fouquet, M.; Baron, J.-C.; Mezenge, F.; Landeau, B.; de La Sayette, V.; Viader, F.; Eustache, F.; Desgranges, B.; Chetelat, G. Sequential Relationships Between Grey Matter and White Matter Atrophy and Brain Metabolic Abnormalities in Early Alzheimer's Disease. *Brain* **2010**, *133* (11), 3301–3314.

(5) Prusiner, S. B. Novel Proteinaceous Infectious Particles Cause Scrapie. *Science* **1982**, *216* (4542), 136–144.

(6) Guiroy, D. C.; Williams, E. S.; Yanagihara, R.; Gajdusek, D. C. Topographic Distribution of Scrapie Amyloid-Immunoreactive Plaques in Chronic Wasting Disease in Captive Mule Deer (Odocoileus Hemionus Hemionus). *Acta Neuropathol.* **1991**, *81* (5), 475–478.

(7) Scott, A. C.; Wells, G. A. H.; Stack, M. J.; White, H.; Dawson, M. Bovine Spongiform Encephalopathy: Detection and Quantitation of Fibrils, Fibril Protein (PrP) and Vacuolation in Brain. *Vet. Microbiol.* **1990**, *23* (1–4), 295–304.

(8) Collinge, J.; Palmer, M. S. Prion Diseases. *Curr. Opin. Genet. Dev.* **1992**, *2* (3), 448–454.

(9) Lampert, P.; Gajdusek, D.; Gibbs, C. J. Subacute Spongiform Virus Encephalopathies. Scrapie, Kuru and Creutzfeldt-Jakob Disease: A Review. *Am. J. Pathol.* **1972**, *68* (3), 626–652.

(10) Haase, A. T. The Pathogenesis of Slow Virus Infections : Molecular Analyses. *J. Infect. Dis.* **1986**, *153* (3), 441–447.

(11) Klitzman, R. L.; Alpers, M. P.; Gajdusek, D. C. The Natural Incubation Period of Kuru and the Episodes of Transmission in Three Clusters of Patients. *Neuroepidemiology* **1984**, *3*, 3–20.

(12) Will, R. Variant Creutzfeldt-Jakob Disease. *Folia Neuropathol.* **2004**, *1996*, 77–83.

(13) Medori, R.; Tritschler, H.-J.; LeBlanc, A.; Villare, F.; Manetto, V.; Chen, H. Y.; Xue, R.; Leal, S.; Montagna, P.; Cortelli, P.; et al. Fatal Familial Insomnia, a Prion Disease with a Mutation at Codon 178 of the Prion Protein Gene. *N. Engl. J. Med.* **1992**, *326* (7), 444–449.

(14) Spillantini, M. G.; Schmidt, M. L.; Lee, V. M. Y.; Trojanowski, J. Q.; Jakes, R.; Goedert, M. Alpha-Synuclein in Lewy Bodies. *Nature* **1997**, *388* (3312), 839–840.

(15) Ozansoy, M.; Başak, A. N. Tauopathies: A Distinct Class of Neurodegenerative Diseases. *Balk. J. Med. Genet.* **2008**, *10* (2), 3–14.

(16) Lee, V. M.; Goedert, M.; Trojanowski, J. Q. Neurodegenerative Tauopathies. *Annu. Rev. Neurosci.* **2001**, *24*, 1121–1159.

(17) Ballatore, C.; Lee, V. M.-Y.; Trojanowski, J. Q. Tau-Mediated Neurodegeneration in Alzheimer's Disease and Related Disorders. *Nat. Rev. Neurosci.* **2007**, *8* (9), 663–672.

(18) Alzheimer's Association of America. *2017 Alzheimer's Disease Facts and Figures*; **2017**.

(19) Williams, D. R.; Silva, R. De; Paviour, D. C.; Pittman, A.; Watt, H. C.; Kilford, L.; Holton, J. L.; Revesz, T.; Lees, A. J. Characteristics of Two Distinct Clinical Phenotypes in Pathologically Proven Progressive Supranuclear Palsy: Richardson's Syndrome and PSP-Parkinsonism. *Brain* **2005**, *128*, 1247–1258.

(20) Tanzi, R. E.; Bertram, L. Twenty Years of the Alzheimer's Disease Amyloid Hypothesis: A Genetic Perspective. *Cell* **2005**, *120* (4), 545–555.

(21) Mez, J.; Daneshvar, D. H.; Kiernan, P. T.; Abdolmohammadi, B.; Alvarez, V. E.; Huber, B. R.; Alosco, M. L.; Solomon, T. M.; Nowinski, C. J.; McHale, L.; et al. Clinicopathological Evaluation of Chronic Traumatic Encephalopathy in Players of American Football. *J. Am. Med. Assoc.* **2017**, *318* (4), 360–370.

(22) Mann, D. M. A. The Pathological Association Between Down Syndrome and Alzheimer Disease. *Mech. Ageing Develppment* **1988**, *43*, 99–136.

(23) Goedert, M.; Spillantini, M. G.; Cairns, N. J.; Crowther, R. A. Tau-Proteins of Alzheimer Paired Helical Filaments - Abnormal Phosphorylation of All 6 Brain Isoforms. *Neuron* **1992**, *8* (1), 159–168.

(24) Goedert, M.; Spillantini, M. G.; Jakes, R.; Rutherford, D.; Crowther, R. A. Multiple Isoforms of Human Microtubule-Associated Protein Tau: Sequences and Localization in Neurofibrillary Tangles of Alzheimer's Disease. *Neuron* **1989**, *3* (4), 519–526.

(25) Himmler, A.; Drechsel, D.; Kirschner, M. W.; Martin, D. W. Tau Consists of a Set of Proteins with Repeated C-Terminal Microtubule-Binding Domains and Variable N-Terminal Domains. *Mol. Cell. Biol.* **1989**, *9* (4), 1381–1388.

(26) Lee, G.; Neve, R. L.; Kosik, K. S. The Microtubule Binding Domain of Tau Protein. *Neuron* **1989**, *2* (6), 1615–1624.

(27) Hirokawa, K.; Shiomura, Y.; Okabe, S. Tau Proteins: The Molecular Structure and Mode of Binding on Microtubules. *J. Cell Biol.* **1988**, *107* (October), 1449–1459.

(28) Goedert, M.; Crowther, R. A.; Garner, C. C. Molecular Characterization of Microtubule-Associated Proteins Tau and MAP2. *Trends Neurosci.* **1991**, *25* (6), 193–199.

(29) Kampers, T.; Friedhoff, P.; Biernat, J.; Mandelkow, E. M.; Mandelkow, E. RNA Stimulates Aggregation of Microtubule-Associated Protein Tau into Alzheimer-like Paired Helical Filaments. *FEBS Lett.* **1999**, *399* (3), 344–349.

(30) Sugino, E.; Nishiura, C.; Minoura, K.; In, Y.; Sumida, M.; Taniguchi, T.; Tomoo, K.; Ishida, T. Three-/four-Repeat-Dependent Aggregation Profile of Tau Microtubule-Binding Domain Clarified by Dynamic Light Scattering Analysis. *Biochem. Biophys. Res. Commun.* **2009**, *385* (2), 236–240.

(31) Barghorn, S.; Biernat, J.; Mandelkow, E. Purification of Recombinant Tau Protein and Preparation of Alzheimer-Paired Helical Filaments in Vitro. In *Amyloid Proteins: Methods in Molecular Biology* **2005**, *299*, 35–51.

(32) Schweers, O.; Mandelkow, E. M.; Biernat, J.; Mandelkow, E. Oxidation of Cysteine-322 in the Repeat Domain of Microtubule-Associated Protein Tau Controls the In Vitro Assembly of Paired Helical Filaments. *Proc. Natl. Acad. Sci. U. S. A.* **1995**, *92* (18), 8463–8467.

(33) Kuret, J.; Congdon, E. E.; Li, G.; Yin, H.; Yu, X.; Zhong, Q. Evaluating Triggers and Enhancers of Tau Fibrillization. *Microsc. Res. Tech.* **2005**, *67*, 141–155.

(34) Goedert, M.; Jakes, M.; Spillantini, M. G.; Hasegawa, M.; Smith, M. J.; Crowther, R. A. Assembly of Microtubule-Associated Protein Tau into Alzheimer-like Filaments Induced by Sulphated Glycosaminoglycans. *Nature* **1996**, *383*, 550–553.

(35) Berriman, J.; Serpell, L. C.; Oberg, K. A.; Fink, A. L.; Goedert, M.; Crowther, R. A. Tau Filaments from Human Brain and from in Vitro Assembly of Recombinant Protein Show Cross-Beta Structure. *Proc. Natl. Acad. Sci. U. S. A.* **2003**, *100* (15), 9034–9038.

(36) Margittai, M.; Langen, R. Template-Assisted Filament Growth by Parallel

Stacking of Tau. *Proc. Natl. Acad. Sci.* **2004**, *101* (28), 10278–10283.

(37) Siddiqua, A.; Margittai, M. Three- and Four-Repeat Tau Coassemble into Heterogeneous Filaments: An Implication for Alzheimer Disease. *J. Biol. Chem.* **2010**, *285* (48), 37920–37926.

(38) Lewis, S. A.; Villasante, A.; Sherline, P.; Cowan, N. J. Brain-Specific Expression of MAP2 Detected Using a Cloned cDNA Probe. *J. Cell Biol.* **1986**, *102* (6), 2098–2105.

(39) Johnson, G. V. W.; Jope, R. S. The Role of Microtubule-Associted Protein 2 (MAP2) in Neuronal Growth, Placticity, and Degeneration. *J. Neurosci. Res.* **2004**, *33* (4), 505–512.

(40) Lewis, S.; Wang, D.; Cowan, N. Microtubule-Associated Protein MAP2 Shares a Microtubule Binding Motif with Tau Protein. *Science* **1988**, *242* (4880), 936–939.

(41) Kalcheva, N.; Albala, J.; O'Guin, K.; Rubino, H.; Garner, C.; Shafit-Zagardo, B. Genomic Structure of Human Microtubule-Associated Protein 2 (MAP-2) and Characterization of Additional MAP-2 Isoforms. *Proc. Natl. Acad. Sci. U. S. A.* **1995**, *92* (24), 10894–10898.

(42) Selkoe, D. J. The Cell Biology of Beta-Amyloid Precursor Protein and Presenilin in Alzheimer's Disease. *Trends Cell Biol.* **1998**, *8* (11), 447–453.

(43) Spillantini, M. G.; Goedert, M. Tau Pathology and Neurodegeneration. *Lancet Neurol.* **2013**, *12* (6), 609–622.

(44) Sergeant, N.; Wattez, A.; Delacourte, A. Neurofibrillary Degeneration in Progressive Supranuclear Palsy and Corticobasal Degeneration: Tau Pathologies with Exclusively "Exon 10" Isoforms. *J. Neurochem.* **1999**, *72* (3), 1243–1249.

(45) Braak, H.; Braak, E. Staging of Alzheimer's Disease-Related Neurofibrillary Changes. *Neurobiol. Aging* **1995**, *16* (3), 271–278.

(46) Nagy, Z.; Esiri, M. M.; Jobst, K. A.; Morris, J. H.; King, E. M. F.; McDonlad, B.; Litchfield, S.; Smith, A.; Barneston, L.; Smith, A. D. Relative Roles of Plaques and Tangles in the Dementia of Alzheimer's Disease: Correlations Using Three Sets of Neuropathological Criteria. *Dement. Geriatr. Cogn. Disord.* **1995**, *6*, 21–31.

(47) Dujardin, S.; Lecolle, K.; Caillierez, R.; Begard, S.; Zommer, N.; Lachaud, C.; Carrier, S.; Dufour, N.; Auregan, G.; Winderickx, J.; et al. Neuron-to-Neuron Wild-Type Tau Protein Transfer through a Trans-Synaptic Mechanism: Relevance to Sporadic Tauopathies. *Acta Neuropathol Commun* **2014**, *2*, 1-14.

(48) Kfoury, N.; Holmes, B. B.; Jiang, H.; Holtzman, D. M.; Diamond, M. I. Trans-Cellular Propagation of Tau Aggregation by Fibrillar Species. *J. Biol. Chem.* **2012**, *287* (23), 19440–19451.

(49) Calafate, S.; Buist, A.; Miskiewicz, K.; Vijayan, V.; Daneels, G.; de Strooper, B.; de Wit, J.; Verstreken, P.; Moechars, D. Synaptic Contacts Enhance Cell-to-Cell Tau Pathology Propagation. *Cell Rep.* **2015**, *11* (8), 1176–1183.

(50) Gelaye, B.; Rondon, M.; Araya, P. R.; A, P. M. Neuronal Activity Enhances Tau Propagation and Tau Pathology in Vivo. *Nat. Neurosci.* **2016**, *3* (10), 973–982.

(51) Josephs, K. A.; Petersen, R. C.; Knopman, D. S.; Boeve, B. F.; Whitwell, J. L.; Duffy, J. R.; Parisi, J. E.; Dickson, D. W. Clinicopathologic Analysis of Frontotemporal and Corticobasal Degenerations and PSP. *Neurology* **2006**, *66* (1), 41–48.

(52) Maldonado, H.; Ramírez, E.; Utreras, E.; Pando, M. E.; Kettlun, A. M.; Chiong, M.; Kulkarni, A. B.; Collados, L.; Puente, J.; Cartier, L.; et al. Inhibition of Cyclin-Dependent Kinase 5 but Not of Glycogen Synthase Kinase 3-β Prevents Neurite Retraction and Tau Hyperphosphorylation Caused by Secretable Products of Human T-Cell Leukemia Virus Type I-Infected Lymphocytes. *J. Neurosci. Res.* **2011**, *89* (9), 1489–1498.

(53) Goedert, M.; Jakes, R.; Vanmechelen, E. Monoclonal Antibody AT8 Recognises Tau Protein Phosphorylated at Both Serine 202 and Threonine 205. *Neurosci. Lett.* **1995**, *189* (3), 167–170.

(54) Otvos Jr., L.; Feiner, L.; Lang, E.; Szendrei, G. I.; Goedert, M.; Lee, V. M.-Y. Monoclonal Antibody PHF-1 Recognizes Tau Protein Phosphorylated at Serine Residues 296 and 404. *J. Neurosci. Res.* **1994**, *39* (6), 669–673.

(55) Saidi, L. J.; Polydoro, M.; Kay, K. R.; Sanchez, L.; Mandelkow, E. M.; Hyman, B. T.; Spires-Jones, T. L. Carboxy Terminus Heat Shock Protein 70 Interacting Protein Reduces Tau-Associated Degenerative Changes. *J. Alzheimer's Dis.* **2015**, *44* (3), 937–947.

(56) Frid, P.; Anisimov, S. V.; Popovic, N. Congo Red and Protein Aggregation in Neurodegenerative Diseases. *Brain Res. Rev.* **2007**, *53* (1), 135–160.

(57) Groenning, M.; Olsen, L.; van de Weert, M.; Flink, J. M.; Frokjaer, S.; Jorgensen, F. S. Study on the Binding of Thioflavin-T to Beta-Sheet-Rich and Non-Beta-Sheet Cavities. *J. Struct. Biol.* **2007**, *158* (3), 358–369.

(58) Voropai, E. S.; Samtsov, M. P.; Kaplevskii, K. N.; Maskevich, A. A.; Stepuro, V. I.; Povarova, O. I.; Kuznetsova, I. M.; Turoverov, K. K.; Fink, A. L.; Uverskii, V.

N. Spectral Properties of Thioflavin T and Its Complexes with Amyloid Fibrils. *J. Appl. Spectrosc.* **2003**, *70* (6), 868–874.

(59) Bergen, M. Von; Friedhoff, P.; Schneider, a; Kampera, T.; Biernat, J.; Mandelkow, E. M.; Mandelkow, E. Rapid Assembly of Microtubule-Associated Protein Tau into Alzheimer-like Paired Helical Filaments Monitored by Fluorescence in Solution. *Mol. Biol. Cell* **1998**, *9* (98), 10223-10230.

(60) Dinkel, P. D.; Holden, M. R.; Matin, N.; Margittai, M. RNA Binds to Tau Fibrils and Sustains Template-Assisted Growth. *Biochemistry* **2015**, *54* (30), 4731–4740.

(61) Guo, C.; Wang, B.; Wang, L.; Xu, B. Structural Basis of Single Molecular Heparin-FX06 Interaction Revealed by SPM Measurements and Molecular Simulations. *Chem. Commun.* **2012**, *48* (100), 12222–12224.

(62) Watson, J. D.; Crick, F. H. C. Molecular Structure of Nucleic Acids. *Nature* **1953**, *171*, 737–738.

(63) Zuker, M. On Finding All Suboptimal Foldings of an RNA Molecule. *Science* **1989**, *244* (4900), 48–52.

(64) Saborio, G. P.; Permanne, B.; Soto, C. Sensitive Detection of Pathological Prion Protein by Cyclic Amplification of Protein Misfolding. *Nature* **2001**, *411* (6839), 810–813.

(65) Soto, C.; Anderes, L.; Suardi, S.; Cardone, F.; Castilla, J.; Frossard, M. J.; Peano, S.; Saa, P.; Limido, L.; Carbonatto, M.; et al. Pre-Symptomatic Detection of Prions by Cyclic Amplification of Protein Misfolding. *FEBS Lett.* **2005**, *579* (3), 638–642.

(66) Meyer, V.; Dinkel, P. D.; Rickman Hager, E.; Margittai, M. Amplification of Tau Fibrils from Minute Quantities of Seeds. *Biochemistry* **2014**, *53* (36), 5804–5809.

(67) Atarashi, R.; Sano, K.; Satoh, K.; Nishida, N. Real-Time Quaking-Induced Conversion. *Prion* **2011**, *5* (3), 150–153.

(68) Ambadipudi, S.; Biernat, J.; Riedel, D.; Mandelkow, E.; Zweckstetter, M. Liquid–liquid Phase Separation of the Microtubule-Binding Repeats of the Alzheimer-Related Protein Tau. *Nat. Commun.* **2017**, *8* (275), 1-13.

(69) Deleault, N. R.; Harris, B. T.; Rees, J. R.; Supattapone, S. Formation of Native Prions from Minimal Components in Vitro. *Proc. Natl. Acad. Sci. U. S. A.* **2007**, *104* (23), 9741–9746.

(70) Meisl, G.; Yang, X.; Hellstrand, E.; Frohm, B.; Kirkegaard, J. B.; Cohen, S. I. A.;

Dobson, C. M.; Linse, S.; Knowles, T. P. J. Differences in Nucleation Behavior Underlie the Contrasting Aggregation Kinetics of the Aβ40 and Aβ42 Peptides. *Proc. Natl. Acad. Sci.* **2014**, *111* (26), 9384–9389.

(71) Raman, B.; Chatani, E.; Kihara, M.; Ban, T.; Sakai, M.; Hasegawa, K.; Naiki, H.; Rao, C. M.; Goto, Y. Critical Balance of Electrostatic and Hydrophobic Interactions Is Required for β2-Microglobulin Amyloid Fibril Growth and Stability. *Biochemistry* **2005**, *44* (4), 1288–1299.

(72) Barghorn, S.; Mandelkow, E. Toward a Unified Scheme for the Aggregation of Tau into Alzheimer Paired Helical Filaments. *Biochemistry* **2002**, *41* (50), 14885–14896.

(73) Meyer, V.; Holden, M. R.; Weismiller, H. A.; Eaton, G. R.; Eaton, S. S.; Margittai, M. Fracture and Growth Are Competing Forces Determining the Fate of Conformers in Tau Fibril Populations. *J. Biol. Chem.* **2016**, *291* (23), 12271–12281.

(74) Fitzpatrick, A. W. P.; Falcon, B.; He, S.; Murzin, A. G.; Murshudov, G.; Garringer, H. J.; Crowther, R. A.; Ghetti, B.; Goedert, M.; Scheres, S. H. W. Cryo-EM Structures of Tau Filaments from Alzheimer's Disease. *Nature* **2017**, *547* (7662), 185–190.

(75) Zhong, Q.; Congdon, E. E.; Nagaraja, H. N.; Kuret, J. Tau Isoform Composition Influences Rate and Extent of Filament Formation. *J. Biol. Chem.* **2012**, *287* (24), 20711–20719.

(76) Dinkel, P. D.; Siddiqua, A.; Huynh, H.; Shah, M.; Margittai, M. Variations in Filament Conformation Dictate Seeding Barrier between Three- and Four-Repeat Tau. *Biochemistry* **2011**, *50* (20), 4330–4336.

(77) Perry, G.; Kawai, M.; Tabaton, M.; Onorato, M.; Mulvihill, P.; Richey, P.; Morandi, A.; Connolly, J. A.; Gambettil, P. Neuropil Threads of Alzheimer's Disease Show a Marked Alteration of the Normal Cytoskeleton. *J. Neurosci.* **1991**, *17* (6), 1746–1755.

(78) Morrison, L. D.; Kish, S. J. Brain Polyamine Levels Are Altered in Alzheimer's Disease. *Neurosci. Lett.* **1995**, *197*, 5–8.

(79) Buée, L.; Delacourte, A. Comparative Biochemistry of Tau in Progressive Supranuclear Palsy, Corticobasal Degeneration, FTDP-17 and Pick's Disease. *Brain Pathol.* **1999**, *9*, 681–693.

(80) Williams, D. R.; De Silva, R.; Paviour, D. C.; Pittman, A.; Watt, H. C.; Kilford, L.; Holton, J. L.; Revesz, T.; Lees, A. J. Characteristics of Two Distinct Clinical

Phenotypes in Pathologically Proven Progressive Supranuclear Palsy: Richardson's Syndrome and PSP-Parkinsonism. *Brain* **2005**, *128* (6), 1247–1258.

(81) Caffrey, T. M.; Joachim, C.; Paracchini, S.; Esiri, M. M.; Wade-Martins, R. Haplotype-Specific Expression of Exon 10 at the Human MAPT Locus. *Hum. Mol. Genet.* **2006**, *15* (24), 3529–3537.

(82) Woerman, A. L.; Aoyagi, A.; Patel, S.; Kazmi, S. A.; Lobach, I.; Grinberg, L. T.; McKee, A. C.; Seeley, W. W.; Olson, S. H.; Prusiner, S. B. Tau Prions from Alzheimer's Disease and Chronic Traumatic Encephalopathy Patients Propagate in Cultured Cells. *Proc. Natl. Acad. Sci.* **2016**, *113* (50), 8187–8196.

(83) Fiandaca, M. S.; Kapogiannis, D.; Mapstone, M.; Boxer, A.; Schwartz, J. B.; Abner, E. L.; Petersen, R. C.; Federoff, H. J.; Miller, B. L.; Goetzl, E. J.; et al. Identification of Pre-Clinical Alzheimer's Disease by a Profile of Pathogenic Proteins in Neurally-Derived Blood Exosomes: A Case-Control Study. *Alzheimer's Dement. J. Alzheimer's Assoc.* **2015**, *11* (6), 600–607.

(84) Salido-Guadarrama, I.; Romero-Cordoba, S.; Peralta-Zaragoza, O.; Hidalgo-Miranda, A.; Rodríguez-Dorantes, M. MicroRNAs Transported by Exosomes in Body Fluids as Mediators of Intercellular Communication in Cancer. *Onco. Targets. Ther.* **2014**, *7*, 1327–1338.

(85) Hamlett, E. D.; Goetzl, E. J.; Ledreux, A.; Vasilevko, V.; Boger, H. A.; LaRosa, A.; Clark, D.; Carroll, S. L.; Carmona-Iragui, M.; Fortea, J.; et al. Neuronal Exosomes Reveal Alzheimer's Disease Biomarkers in Down Syndrome. *Alzheimer's Dement.* **2017**, *13* (5), 541–549.